Aus Institut für Pathobiochemie
der Universitätsmedizin der Johannes Gutenberg-Universität Mainz

Investigation of the effect of reversible NMDA receptor blockade in vivo on the expression and phosphorylation status of the microtubule-associated protein tau

Untersuchung der Auswirkungen einer reversiblen Blockade von NMDA-Rezeptoren in vivo auf die Expression und den Phosphorylierungsstatus des Mikrotubuli-assoziierten Proteins Tau

Inauguraldissertation
zur Erlangung des Doktorgrades der
Medizin
der Universitätsmedizin
der Johannes Gutenberg-Universität Mainz

Vorgelegt von

Alan Souid
aus Homs

Mainz, 2025

Wissenschaftlicher Vorstand: Univ.-Prof. Dr. med. Philipp Drees

1. Gutachter: Univ.-Prof. Dr. Bernd Moosmann

2. Gutachter: Prof. Dr. rer. nat. Kristina Endres

Tag der Promotion: 21. Oktober 2025

Nachnutzungslizenz: CC-BY-4.0

Table of Contents

List of Figures

List of Tables

List of Abbreviations

(+)-5-Methyl-lo,1l-dihydro-5H-dibenzo[a,d]cyclohepten-5,10-imine maleate (MK-801).

2-(4-(2-Hydroxyethyl)-1-piperazinyl)-ethansulfonsäure (HEPES)

2-Amino-7-phosphono-hepatonate (APH).

4-(3-Phosphonopropyl)-2-piperazinecarboxylic acid (CCP).

Amyloid precursor protein (APP).

Amyloid-ß Aß.

Bicinchoninic acid (BCA).

Bovine serum albumin (BSA).

Calcium chloride ($CaCl_2$).

Calmodulin-dependent kinase (CaMK).

Cyclic adenosine monophosphate (cAMP).

cAMP response element binding (CREP).

Cornu ammonis (CA).

Cyclin dependent kinase-5 (CDK-5).

Cyclin-dependent kinase 2 (CDK-2).

Dentate gyrus (DG).

Dimethyl sulfoxide (DMSO)

Early-onset Alzheimer´s Diosease (EOAD).

Entorhinal cortical (EC).

Ethylenediamine tetraacetic acid (EDTA)

GABA (gamma aminobutyric acid).

Glycogen synthase kinase-3ß (GSK-3ß).

Hydrogen chloride (HCl)

Intraperitoneal (i.p)

Individual registration number (IRN).

Kilodalton (KDa).

Late-onset Alzheimer´s Disease (LOAD).

Long-time potentiation (LTP).

Magnesium chloride ($MgCl_2$).

Mild cognitive impairment or MCI.

Mini Mental State Examination (MMSE).

Minute (min).

Hour (h).

Mitogen-activated protein kinase (MAPK).

Neurofibrillary tangles (NFTs).

intra-neuronal neurofibrillary tangles (iNFT).

extra-neuronal neurofibrillary tangles (eNFT).

Neuropil threads (NTs).

N-Methyl-D-aspartate receptor (NMDA receptor).

Paired helical filament (PHF).

Phencyclidine (PCP).

Postsynaptic density protein (PSD-95).

Posterior cingulate cortex (PCC).

Potassium chloride (KCl)

Presenilin-1 (PS1).

Retrosplenial cortex (RCC).

SDS-PAGE (sodium dodecyle sulfate-polyacrylamide gel electrophoresis).

Sodium chloride (NaCl).

Sodium dihydrogen phosphate (NaH_2PO_4).

Sodium fluoride (NaF).

Sodium orthovanadate (Na3VO4).

ß-site APP cleaving enzyme (BACE).

Standard Operating Procedures (SOPs).

Subiculum (SUB).

Tris-Buffered Saline (TBS).

Traumatic Brain Injury (TBI).

Tris(hydroxymethyl)aminomethan (TRIS).

Volt (V).

1 Introduction

1.1 Alzheimer´s Disease: Definition and Epidemiology

Alzheimer´s disease is a neurodegenerative disorder associated with progressive deterioration of cognition and memory (Selkoe 2001). Alzheimer´s disease was described originally by Alois Alzheimer and Oskar Fischer (Alzheimer 1907; Fischer 1907). Some patients manifest early symptoms long time before a clinical diagnosis of dementia. These symptoms include mood, anxiety, and sleep changes. Anxiety, depressive symptoms, apathy, and withdrawal are common in the early stages of Alzheimer´s disease (Farlow and Cummings 2007; Jost and Grossberg 1995; Jost and Grossberg 1996).

The prevalence of Alzheimer´s disease rises with age; while just 3% of people between 65 and 75 have Alzheimer´s disease, 17% of people between 75 and 84, and 32% of people older than 84 are affected by the disease (Alzheimer´s Association 2019). The prevalence of Alzheimer´s disease doubles approximately every 5 years for people between the age of 65 and 85 (Alzheimer's Association 2018). Advancing aging is not the only risk factor for Alzheimer´s disease; other prominent risk factors are family history, Apolipoprotein E ε4, cardiovascular disease risk factors, head trauma, traumatic brain injury and mild cognitive impairment (MCI) (Alzheimer´s Association 2011). In the age group of 64 and older, about 15%-20% of people have MCI, and about 15% of them develop dementia within 2 years (Petersen et al., 2018). People with amnestic MCI show a higher tendency to develop Alzheimer´s disease or related dementia (Lopez et al., 2019). Younger age, higher education, better global cognition, as measured by the Mini Mental State Examination (MMSE), and fewer neuropsychiatric symptoms are associated with a high probability of returning from MCI to a normal state (Sugarman et al., 2018).

Based on age there are two subtypes of Alzheimer´s disease: early-onset Alzheimer´s disease (EOAD) and late-onset Alzheimer´s disease (LOAD). Early-onset Alzheimer´s disease is responsible for approximately 1% to 6% of all cases, and the age of patients with EOAD varies from 30 to 60 or 65. However, the most common form of Alzheimer´s disease (LOAD) occurs in patients older than 60 or 65 (Bekris et al., 2010).

Autosomal dominant gene mutations, especially mutations in these separate three genes (APP, Presenilin 1, and Presenilin 2) can be responsible for early onset Alzheimer´s disease (EOAD) (Lopez et al., 2019). However, 37% of LOAD are associated with mutations in the

Apolipoprotein E gene (Lambert et al., 2013).

1.2 Neuropathology of Alzheimer´s Disease

The two main characteristic protein deposits of Alzheimer´s disease are extracellular amyloid plaques and intracellular neurofibrillary tangles (NFTs). The NFTs form because of hyperphosphorylation and aggregation of the tau protein (Selkoe 2001; Mielke et al., 2014). Amyloid ß (Aß), which plays a major role in amyloid plaque formation, originates from Amyloid-ß precursor protein (APP) by proteolytic cleavage (Haass et al., 1992; Selkoe 1997). Aß formation is prevented by cleavage of APP within the Aß domain of APP (α-cleavage), whereas sequential cleavage of the N and C termini of the Aß domain of APP (ß-cleavage and γ-cleavage) causes Aß formation (Haass 2004; Kojro and Fahrenholz 2005). It was determined that members of the metalloproteinase and disintegrin families were involved in the α-cleavage; the ß-cleavage is mediated by the ß-site APP cleaving enzyme (BACE), whereas presenilin-1 (PS1), nicastrin, anterior-pharynx deficient protein-1, and presenilin enhancer-2 coordinate the γ-cleavage of APP (Stokin and Goldstein 2006). Tau is originally a microtubule (MT-)binding protein. Its binding to MTs is controlled by phosphorylation at multiple sites (Sengupta 1998). One of the known functions of the tau protein is regulation of MT stability and MT-dependent processes (Ittner et al., 2010). Tau protein can be phosphorylated at different sites in the N-Terminal region, the repeat region, and the C-Terminal region (Zhang et al., 2021). Many enzymes induce phosphorylation on these sites, including protein kinase A (PKA), protein kinase C (PKC), cyclin dependent kinase-5 (CDK-5), glycogen synthase kinase-3ß (GSK-3ß), and mitogen-activated protein kinase (MAPK) (Zheng et al., 2002; Singh et al., 1995). These kinases play a role in the hyperphosphorylation of the tau protein in pathological conditions, which results in tau protein dissociating from MTs and forming NFTs (Zhang et al., 2021). Therefore, in Alzheimer´s disease, the hyperphosphorylation of tau leads to the accumulation of tau aggregates, forming NFTs and neuropil threads (NTs) (Geschwind 2003). The other major protein in Alzheimer's disease, amyloid ß, plays a physiological role in normal healthy brains too, potentially improving learning and memory formation (Crystal 2020; Garcia-Osta and Alberini 2009; Morley and Farr 2014). In contrast, the accumulation of high levels of Aß and aggregate formation, like in Alzheimer´s disease, causes cognitive dysfunction and memory deficits (Haass and Selkoe 2007). Some studies suggested an interaction pathway between Aß and tau, which contributes to the pathological process of Alzheimer´s disease (Iijima et al., 2010; Grundke-Iqbal et al., 1986).

According to the "Aß Cascade Hypothesis", Aß, which is deposited as neurotic plaques, causes Alzheimer´s disease by harming neuronal cells (Selkoe 2008). Furthermore, some studies hypothesize that Aß speeds up tau phosphorylation via CDK-5 (Hernandez et al., 2009) and GSK-3ß (Terwel et al., 2008). However, substantial evidence has emerged in the last

years questioning this idea and suggesting that Aß and tau pathology are caused at the same time by associated but independent mechanisms. One evidence is the finding that Aβ and tau pathology initially start in different brain regions; tau pathology starts in the (trans)entorhinal cortex and spreads to limbic areas, and finally to the neocortex during progression to Alzheimer´s disease dementia. On the contrary, Aβ pathology develops in the association cortices and spreads from neocortex to allocortex (van der Kant, Goldstein, and Ossenkoppele 2020). Furthermore, the analysis of the human brain of Alzheimer´s disease patients postmortem has shown that the tau pathology started in some areas of the brain before the Aß cascade (Braak and Braak 1997). In addition, the Tg 2576 mouse model is one of the best characterized and widely used mouse models of Alzheimer´s disease. It overexpresses a mutant form of APP (isoform 695) with the Swedish mutation (Lys670 --> Asn, Met671 --> Leu), resulting in elevated levels of Aβ and ultimately amyloid plaques (Hsiao et al., 1996). The studies on the Tg 2576 mice did not show an increase in tau phosphorylation or development of neurofibrillary tangles in the brains of these mice (Hsiao et al., 1996; Irizarry et al., 1997).

1.3 Early Hallmarks of Alzheimer´s Disease

Even though the clinical symptoms of Alzheimer´s disease appear in advanced age groups, the pathological hallmarks, including extracellular deposits of Aß-amyloid protein and intraneuronal neurofibrillary changes, can manifest at young age over extended periods of time before the appearance of clinical symptoms (Braak and Braak 1997; Braak et al., 1999). Several decades pass between the time a histologically proven transmission first manifests and the illness in which enough damage has been done for clinical symptoms to appear (Ohm et al., 1995; Ohm 1997).

The destructive process of Alzheimer´s disease affects only specific areas, layers, and subcortical nuclei in the human brain. The destructive process starts in predisposed cortical induction sites and spreads to various subcortical nuclei and other regions of the cerebral cortex in a regular and predictable pattern (Braak et al., 1999). There are six stages in the evaluation of the neurofibrillary changes NFT/NT, which can be distinguished postmortem by determining the location of the damaged neurons and the degree of the pathology (Braak and Braak 1991; 1994; 1997; Samuel et al., 1996; Hyman 1998).

The first affected cortical neurons are specific projection cells in the transentorhinal region (temporal lobe) (stage I). First, the lesions then spread into the entorhinal region proper (stage II). After that, the hippocampus and temporal proneocortex are both affected (stage III), then the association areas of the nearby neocortex (stage IV), and finally, the lesions spread into the neocortex (stage V) and extend to the primary areas of the temporal lobe (stage VI) (Braak

1997). Stages V and VI of the illness, which correspond to later stages of Alzheimer´s disease, are typical when patients receive their initial diagnosis from doctors (Figure 1) (Braak et al., 1999).

Aside from affecting particular regions, layers and subcortical nuclei, Alzheimer´s disease 's destructive process also only targets a small subset of the vast variety of nerve cell types found in the human brain (Hyman and Gomez-Isala 1994). It was found that the order of NFT/NT appearance during Alzheimer´s disease development bears a striking resemblance to the inverse order of cortical myelination. Late myelinating cortical areas and layers develop NFTs and NTs sooner and at higher densities than those that begin myelination early (McGeer et al., 1990; Braak and Braak 1996; Braak et al., 1999). Recent studies show that intraneuronal formation of pretangle material can be seen in the lower brainstem nuclei with projections to the cerebral cortex before the NFT changes in the transentorhinal region. These pretangle changes may start before puberty or in early young adulthood (Braak et al., 2011).

Tau phosphorylation and aggregation were also studied in the fetal human brain. One study shows that hyperphosphorylated tau with epitopes that overlap with, but are not identical to, those observed in Alzheimer´s disease are present in the developing fetal brain. Notably, four serine sites (Ser214, Ser396, Ser404, and Ser202) seem to be phosphorylated in both scenarios (Hefti et al., 2019). A deeper comprehension of the phosphorylation of tau during fetal brain development could help to understand the mechanism of triggering toxic tau aggregation and lead to the discovery of potential therapeutic targets for Alzheimer´s disease and other neurodegenerative diseases.

These early hallmarks of Alzheimer's pathology support the idea that Alzheimer´s disease does not begin at old age and is not a natural part of normal aging. Rather, the disease's mechanism starts at an earlier age and can likely be influenced by a variety of factors throughout life.

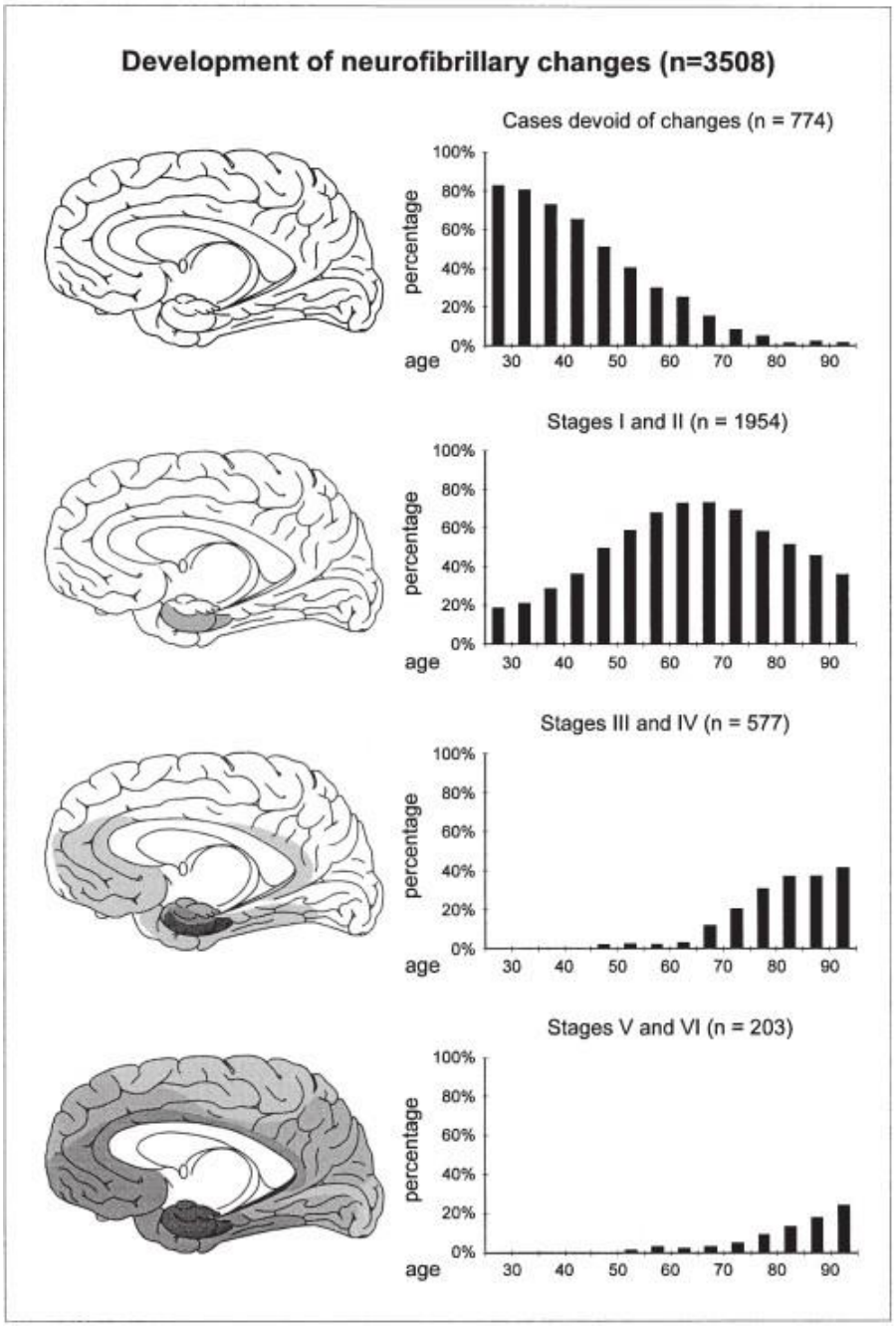

Figure1: Evolution of neurofibrillary changes in a total number of 3508 non-selected autopsy cases.

The first graph presents the percentage of cases without neurofibrillary changes in relation to the total number of cases within each age category. Some people develop lesions corresponding to transentorhinal stages I/II early in life (second graph). Thus, old age is not an essential requirement for the initiation of degenerative changes. The third graph shows cases of the limbic stages III/IV, and the fourth graph those with fully developed Alzheimer´s disease (neocortical stages V/VI). Note that early stages happen primarily in younger age categories, while more advanced stages slowly emerge with increasing age (Braak et al., 1999).

1.4 Axonal Transport and the Pathology of Alzheimer´s Disease

The movement of proteins and vesicles between cell bodies and presynaptic sites is severely challenged by extraordinary length of some axons of the neuronal cells in the human body, which can reach lengths of over 1 m. Axons and dendrites depend on a specialized transport machinery made of cytoskeletal motor proteins to overcome this challenge (Stokin and Goldstein 2006; Hajieva and Moosmann 2015). These proteins produce directed movements along cytoskeletal tracks (Stokin and Goldstein 2006). Motor proteins such as kinesin and dynein transport the proteins along the microtubules. While kinesins play a central role in anterograde axonal transport, dyneins are responsible for retrograde axonal transport. Many proteins implicated in the pathogenesis of Alzheimer's disease (including APP, PS1, ß-site APP cleaving enzyme (BACE), synuclein, and tau) have been discovered in the axonal compartment of neurons, with many of them found at presynaptic terminals (Siman and Salidas 2004; Capell et al., 2002; Beher et al., 1999; Iwai et al., 1995).

Many proteins implicated in the pathogenesis of Alzheimer´s disease have functions in axonal growth. This idea is supported by a wealth of evidence. APP plays an important role in axonal regeneration, and research on the biological roles of APP suggested a potential function in encouraging axonal growth (Masliah et al., 1992; Nicolas and Hassan 2014). There is evidence that APP plays a role in the preservation of axonal structure and function because both APP deletions (Magara et al., 1999) and APP overexpression (Gonzalez-Lima et al., 2001) resulted in reductions in the white matter of the brain in mice. Furthermore, Drosophila experiments suggest a role for the Drosophila APP-like (APPL) gene in brain injury recovery (Leyssen et al., 2005). Similar to APP, PS1 manipulations in cell culture systems show a role in axonal growth and morphology (Furukawa et al., 1998), which has been demonstrated to be crucial in states of axonal injury (Chen et al., 2004). Although there is less information available on BACE, its overexpression causes overt axonal degeneration (Rockenstein et al., 2005) and reduces APP axonal transport (Lee et al., 2005). These proteins (APP, PS1) need to be adequately transported to their final destinations (Koo et al., 1990). Convincing evidence for the role of kinesin-1 in the transport of APP has been found in mice (Kamal et al., 2000). Tau has a role in regulating kinesin-1-mediated vesicle trafficking, playing an important function in transporting of APP and PS1, and organelle transport along microtubules as well as organizing axonal microtubules (Ittner et al., 2010; Stokin et al., 2005). Besides its role of transporting APP and other proteins which implicate in Alzheimer´s disease, tau phosphorylation also modulates the function of different neurotransmitter receptors like NMDA receptors, and the transport and activity of these receptors are also regulated by tau phosphorylation (Setou et al., 2000; Ittner et al., 2010). NR2B subunits, which with NR1 subunits form NMDA receptors

are transported by KIF 17, a kinase super family motor protein (Setou et al., 2000). Furthermore, tau protein interacts with the kinase Fyn, which activates NMDA receptors (Ittner et al., 2010).

These findings show the importance of tau protein in axonal transport and neurotransmission and reveal the possible interaction of NMDA receptor and Tau protein.

1.5 NMDA Receptors and their Role in Cognitive Function

The NMDA receptor (NMDA) is a tetramer, which consists of two NR1 subunits and two NR2 subunits, or less commonly, two NR3 subunits. The NR1 subunits have eight isoforms, which are produced by alternative RNA splicing, and there are four subtypes of NR2 subunits (NR2A_D) and two subtypes of NR3 subunits (NR3A_B). Each subtype is produced by a separate gene. The former determines the physiological and pharmacological properties of each tetramer receptor (Benarroch 2011). Each NMDA receptor subunit consists of a large extracellular amino (NH)-terminal domain, three membrane-spanning domains (M1, M3, and M4), a re-entry loop (M2), and an intracellular carboxy (COOH)-terminal domain that has phosphorylation (P) sites (Figure 2) (Bennarroch 2011, Mayer 2006). The NR1 subunits bind glycine or D-serine, and the NR2 subunits bind glutamate (Kalia et al., 2008). Typical NR1/NR2 receptors are permeable to potassium (K^+), sodium (Na^+) and calcium (Ca^{2+}), and binding of 2 molecules of glutamate to the NR2 and 2 molecules of glycine (or D-serine) to the NR1 subunit is necessary to activate the NMDA receptor (Huang et al., 2012, Benarroch 2011).

Ca^{2+} enters the cell after the activation of NMDA receptor, which leads to the phosphorylation of calmodulin-dependent kinase (CaMK) and the cAMP response element binding (CREB) protein. These phosphorylated proteins initiate the transcription of genes needed for long-term potentiation (LTP) formation, the key to memory formation and neuronal plasticity (Huang et al., 2012; Silva 2003). Concisely, the activation of post-synaptic NMDA receptor leads, in most hippocampal pathways, to the initiation of an activity-dependent synaptic modification sustaining LTP (Bliss and Collingridge 1993).

NR1-NR2B complexes in vitro showed longer excitatory postsynaptic potentials than NR1-NR2A complexes, which considers that increasing NR2B subunits into functional receptor complexes in vivo may support the capacity of NMDA receptors to detect synaptic coincidence. Therefore, synaptic efficacy and memory function increase (Newcomer et al., 2000; Monyer et al., 1994). Increased NR2B subunits in the hippocampus can activate LTP and learning (Tang et al., 1999), and on the other hand, a decrease in NR2B-containing receptors may cause impairment of LTP induction and, as a result, decrease memory function and learning (Gardoni et al., 2009).

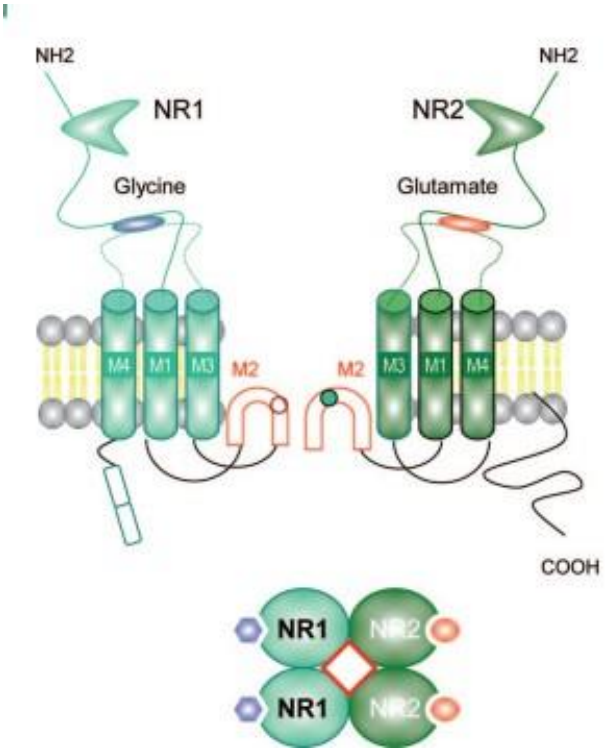

Figure 2: Structure of NMDA receptors.

The NMDA receptors are heteromeric complexes consisting of four subunits stemmed from three related families: NR1, NR2, and NR3. The NR1 is an essential subunit that combines with NR2 or NR3 subunits to make a functional receptor. The typical NMDA receptor requires two NR1 subunits, which bind glycine, and two NR2 subunits, which bind glutamate. Each NMDA receptor subunit includes a large extracellular amino (NH2)-terminal domain (ATD), three membrane-spanning domains (M1, M3, M4), a re-entry or hairpin loop that forms the pore-lining region (M2), and an intracellular carboxy (COOH)- terminal domain that contains phosphorylation (P) sites. The typical NR1/NR2 receptors are permeable to Ca^{2+} and their activation needs the ligation of two molecules of glutamate to the NR2 and two molecules of glycine (or D-serine) to the NR1 subunit (Benarroch 2011).

1.6 NMDA Receptor dysfunction and Alzheimer´s Disease

NMDA receptors are at the heart of learning and memory processes. These functions are severely affected in Alzheimer´s disease. Therefore, it was interesting to study the effect of NMDA receptor blockage towards the molecules that, in aberrant form, define the pathology of Alzheimer´s disease. A relation between NMDA receptor hypofunction and neurodegeneration was first observed when NMDA antagonist drugs were administered to

adult rats, and this treatment reliably caused an injury of the cerebrocortical neurons (Olney, Wozniak, and Farber 1997; Olney, Labruyere and Price 1989). Many studies in animals showed that pharmacological blockade of NMDA function induces defects in memory functions, including impairment in the consolidation of short-term memory into long-term memory (Newcomer, Farber, and Olney 2000). Besides, early studies of the effect of the NMDA noncompetitive antagonist phencyclidine (PCP) (Javitt and Zukin 1991) on cognitive function in humans showed transient, treatment-related reductions in memory performance, psychomotor processing speed, and selective reaction (Rosenbaum et al., 1959, Davies and Beech 1960, Bakker and Amini 1961). Another non-competitive NMDA antagonist, ketamine, triggers at acute subanesthetic doses steady transient decreases in long-term learning and memory performance (Newcomer, Farber, and Olney 2000). This evidence provided dedicated support for the proposal that a decrease in NMDA receptor function can decrease memory and learning functions.

Besides memory dysfunction, treatment with high doses of an NMDA antagonist has shown a pattern of neurodegeneration in the rat brain which was partially similar to the pattern in Alzheimer´s disease by various researchers. The posterior cingulate cortex (PCC) and retrosplenial cortex (RCC) showed neurodegeneration patterns after NMDA receptor blockade that resembled the early stages of Alzheimer´s disease (Olney, Wozniak, and Farber 1997; Minoshima et al., 1997). The Alzheimer´s disease brain and the NMDA receptor hypofunction model showed similar neuronal changes in other brain regions, including portions of the parietal, temporal, entorhinal, and insular cortices (Newcomer, Farber, and Olney 2000). Furthermore, individuals with Alzheimer´s disease or merely mild cognitive impairment show less NMDA receptors expression in the frontal cortex and hippocampus (Procter et al., 1989). One study showed by examination of post-mortem of Alzheimer´s disease patients that NR1/NR2B receptor expression levels in these tissues were reduced with increasing pathological severity (Mishizen-Eberz et al., 2004). In addition, a study on a genetic mouse model of Alzheimer´s disease showed decreased expression of NMDA receptors in neurons (Snyder et al. 2005). However, the decrease of NMDA receptors expression in Alzheimer´s disease could be a result of the loss of neuronal neurons in advanced stages of Alzheimer´s disease, and therefore, the role of NMDA receptors blockade is still unclear. With advancing age, the NMDA receptor becomes hypofunctional (Newcomer, Farber, and Olney 2000). NR1 and NR2B expressions decrease with aging in the cortex and hippocampus of rodents (Magnusson and Simonds 1998; Sheng et al., 1994).

Therefore, the age-related decreases in memory and learning could be due to age-related decreases in NMDA receptor function. In the Alzheimer´s disease brain some risk factors may

promote the hypofunction of NMDA receptors and increase the possibility of neurodegeneration, this could be a main difference between the aging Alzheimer´s disease brain and the aging normal brain (Olney, Wozniak, and Farber 1997).

The same study (Olney, Wozniak, and Farber 1997) suggests that the hypofunction of NMDA receptor can contribute to the formation of NFTs. As already mentioned, some researches have shown that tau engages in transporting NMDA receptor subunits and NMDA receptor activation (Setou et al.,2000; Ittner et al., 2010), which leads to the question if there could be regulatory circuit interaction between NMDA receptors and Tau phosphorylation. Moreover, tau phosphorylation has long been known to be induced after events that non-specifically inhibit excitatory neurotransmission, such as hibernation (Arendt et al., 2003) and traumatic brain injury (TBI) (Edwards et al., 2017; Zanier et al., 2018). Therefore, there could be a connection between blockade of NMDA receptors and their excitatory neurotransmission role and the phosphorylation of the tau protein at different epitopes.

The current study has examined the effect of NMDA receptor inhibition on tau phosphorylation (a hallmark of Alzheimer´s disease) in vivo. It has been investigated whether targeted, pharmacologically induced inhibition of NMDA receptor in the brain of male mice via the non-competitive antagonist MK-801 will influence tau expression and phosphorylation in different areas of the brain.

2 Material and Methods

2.1 Material

2.1.1 Chemicals and Kits

Table 1: List of chemicals in alphabetical order (catalog number if available).

Reagent	**Producer**	**Catalog Number**
2-Mercapthoethanol	Carl Roth (Germany)	4227.3
Acetic acid	Carl Roth (Germany)	6755.2
BCA-Assay	Thermo Fischer Scientific (USA)	23228
Bovine serum albumin	Sigma-Aldrich (USA)	A7906
Bromophenol blue	Sigma-Aldrich (USA)	B-6131
Calcium chloride ($CaCl_2$)	Sigma-Aldrich (USA)	
D (+)-Glucose	Sigma-Aldrich (USA)	
Dimethyl sulfoxide (DMSO)	Sigma-Aldrich (USA)	D4540
Ethanol	VWR Chemicals (Germany)	85033.320
Ethylenediamine tetraacetic acid (EDTA)	Carl Roth (Germany)	8043.2
Glycerol	Sigma-Aldrich (USA)	56815
Glycine	Carl Roth (Germany)	3908.3
Hydrogen chloride (HCl)	Merck (Germany)	100319
Hydrogen peroxide	Sigma-Aldrich (USA)	216763
Imidazole	Sigma-Aldrich (USA)	
Luminol	Sigma-Aldrich (USA)	123072-5G
Magnesium chloride ($MgCl_2$)	Sigma-Aldrich (USA)	
Methanol	VWR Chemicals (Germany)	20903.368
Milk powder	VWR Chemicals (Germany)	3957.2
PagueRuler Prestained Protein Ladder	Thermo Fischer Scientific (USA)	26616
p-Coumaric acid	Sigma-Aldrich (USA)	C9008-5G
PhosSTOP Cocktail Tablets	Hoffmann-La Roche (Switzerland)	04906837001
Ponceau S	Sigma-Aldrich (USA)	P3504

Potassium chloride (KCl)	Carl Roth (Germany)	9781.1
Protease Inhibitor Cocktail	Sigma-Aldrich (USA)	P8340
SDS dust-free pellets	Sigma-Aldrich (USA)	75746
Sodium chloride (NaCl)	Carl Roth (Germany)	A0830
Sodium dihydrogen phosphate (NaH_2PO_4)	Sigma-Aldrich (USA)	
Sodium fluoride (NaF)	Sigma-Aldrich (USA)	
Sodium Orthovanadate	Sigma-Aldrich (USA)	
Tris(hydroxymethyl)aminomethan-Base (TRIS-Base)	Carl Roth (Germany)	4855.2
TRIS-hydrochloride	Carl Roth (Germany)	9090.3
Tween 20	Carl Roth (Germany)	9127.1

2.1.2 Buffers and Solutions

Table 2: Composition of buffers and solutions

Buffer	**Composition**
Tris buffer 1x	100mM Tris/ Tria-HCl pH=7.4
Lysis buffer (not denaturing) 1x	100 mM Tris/Tris-HCl Protease-Inhibitor-Cocktail Phosphatase-Inhibitor-Cocktail pH= 7.4
Lysis buffer (denaturing)	100 mM Tris/Tris-HCl Phosphatase-Inhibitor-Cocktail Protease-Inhibitor-Cocktail 20% Saccharose 0.5% (w/v) SDS pH=7.4
Lysis buffer for 1:3 dilution (denaturing)	100 mM Tris/Tris-HCl 0,75% (w/v) SDS 30% Saccharose Protease-Inhibitor-Cocktail Phosphatase-Inhibitor-Cocktail pH=7.4
Lysis buffer for 1:8 dilution (denaturing)	100 mM Tris/Tris-HCl

	0,55% (w/v) SDS 23% Saccharose Protease-Inhibitor-Cocktail Phosphatase-Inhibitor-Cocktail pH=7.4
Lysis buffer for 1:2 dilution (denaturing)	100 mM Tris/Tris-HCl 1 % (w/v) SDS 40% Saccharose Protease-Inhibitor-Cocktail Phosphatase-Inhibitor-Cocktail pH=7.4
Ringer solution	Preparation of Ringer solution 125 mM NaCl 2,5 mM KCl 1,25 mM NaH_2PO_4 25 mM D (+)-Glucose 1 mM $MgCl_2$ 2 mM $CaCl_2$ 25 mM HEPES pH=7,4 Each time before use were freshly added: 2 mM Imidazole 1 mM NaF 1 mM Na_3VO_4
Loading buffer 4x	48 mM Tris-HCl 152 mM Tris-Base 40% (v/v) Glycerol 20 mM EDTA 0.08% (w/v) Bromophenol blue 8% (w/v) SDS 20% (v/v) 2-Mercaptoethanol pH=6.8
Running buffer 10x	2.5 M Glycine 250 mM Tris-Base 1% (w/v) SDS pH=8.3

Transfer buffer 10x	2.5 M Glycine 250 mM Tris-Base pH=8.3
Transfer buffer 1x	10% (v/v) 10x transfer buffer 20% (v/v) methanol
TBS (Tris-Buffered Saline) 10x	1.37 M NaCl 27 mM KCl 31 mM Tris-Base 217 mM Tris-HCl pH=7.4
TBS-T 1x	TBS 10x diluted 1:10 0.05% (v/v) Tween-20
Ponceau solution	0.2% (w/v) Ponceau S 5% (v/v) Acetic acid
Blocking buffer	5% (w/v) powdered milk in 1x TBS-T
ECL-A	0.1 M TRIS buffer (pH=8.6) 0.05% (v/v) Luminol
ECL-B	0.11% (v/v) p-Coumaric acid in DMSO

2.1.3 Equipment

List of equipment in alphabetical order:

- Amersham Imager from Cytiva (USA).
- Basic Meter PB-11 from Sartorius (Germany).
- Centrifuge 5414 D from Eppendorf (Germany).
- Centrifuge 5424 R from Eppendorf (Germany).
- Criterion Blotter from Bio-Rad Laboratories (USA).
- Criterion Cell from Bio-Rad Laboratories (USA).
- Mini Rocker MR-1 from Biosan (Latvia).
- MR 3001 Magnetic stirring hotplate from Heidolph Instruments (Germany).
- MS2 Minishaker from IKA Works (Germany).
- Multiskan FC from Thermo Fisher Scientific (USA).
- PowerPac HC High-Current Power Supply from Bio-Rad Laboratories (USA).
- ROCKER 2D digital from IKA Works (Germany).

- Thermomixer F1.5 from Eppendorf (Germany).

2.1.4 Antibodies

Table 3: Antibodies used for Western Blotting; antibodies were diluted in TBS-T supplemented with 0.04% NaN_3

Name	Target	Origin	Dilution for Western Blotting	Producer
PHF1	Tau (pSer396, pSer404)	Mouse (mAb)	1:500	Dr. Peter Davies
CP13	Tau (pSer202)	Mouse (mAb)	1:500	Dr. Peter Davies
MAB3420 Tau-1	Tau	Mouse (mAb)	1:2000	EMD Millipore Corp. (USA)
Anti-α-Tubulin MCAP-77	α-Tubulin	Rat (mAb)	1:4000	Serotec (UK)
Anti-α-Tubulin T9026	α-Tubulin	Mouse (mAb)	1:2000	Sigma-Aldrich (USA)
Anti-Mouse IgG 715-035-151	Mouse IgG	Donkey (pAb)	1:10000	Jackson ImmunoResearch
Anti-Rat IgG 712-035-153	Rat IgG	Donkey (pAb)	1:10000	Jackson ImmunoResearch

2.2 Animal Studies

Animal experiments and the preparation of mouse brains were performed by QPS Austria's Neuropharmacology Group (Grambach, Austria). The animal preparation was performed in accordance with the study plan and QPS Austria Standard Operating Procedures (SOPs).

The QPS Austria animal laboratory is certified by the Association for Assessment and Accreditation of Laboratory Animal Care (AAALAC). All procedures adhered to the animal welfare regulations of the Ministry of Science of the Austrian government (TVG 2012).

2.2.1 Accommodation and Housing of Animals

The animals were transported from Janvier Labs in France to QPS Austria, delivered to the assigned animal room, unpacked, and their health status were checked. An animal list was generated, including individual registration number (IRN), date of birth, and sex. Animals were housed in individual ventilated cages, each containg a maximum of four mice. The room temperature was kept at approximately 21°C. Dried, pelleted standard rodent chow (Altromin) as well as normal tap water were available to the animals. Only animals in good health were included in the study. Animals were randomly enclosed in starting groups (cohorts) comprising animals from all testing groups.

2.2.2 Animal Treatments

25 male C57BI/6JRj (Janvier Labs) at the age of ten weeks were randomly allocated to five different treatment groups (Table 4). The mice were treated intraperitoneally (i.p.) with one dose of MK-801 hydrogen maleate (4 groups) or vehicle (1 group).

Table 4: Mouse treatment groups

Group	Test item	Dosage of MK-801	Sampling of time-point	n
A	Vehicle		1 hour	5
B	MK-801	5.0 mg/kg	1 hour	5
C	MK-801	5.0 mg/kg	2 hours	5
D	MK-801	5.0 mg/kg	4 hours	5
E	MK-801	5.0 mg/kg	24 hours	5

One of the mice (IRN 2668, Group D) died prematurely and was substituted.

2.2.3 Tissue Sampling and Sample Shipment

one, two, four or 24 hours after treatment, the mice were sacrificed by cervical dislocation (Table 4). After cervical dislocation, brains were removed and weighed (Table 5) before they were immediately frozen on dry ice and stored at -80°C until shipment.

The fresh frozen brains were shipped at -80°C to the Institute of Pathobiochemistry, University medical center in Mainz.

Table 5: Animal list with brain weight (g)

Group	IRN	Brain weight (g)
A	2638	0.4263
A	2652	0.4535
A	2658	0.4395
A	2678	0.4641
A	2686	0.4418
B	2640	0.4656
B	2666	0.4504
B	2670	0.4368
B	2676	0.4469
B	2688	0.4306
C	2646	0.4506
C	2648	0.4504
C	2662	0.4295
C	2682	0.4386
C	2690	0.4274
D	2644	0.4359
D	2656	0.467
D	2668	0.4214
D	2672	0.4488
D	2692	0.4152
E	2636	0.3999
E	2650	0.4503
E	2674	0.4503
E	2684	0.4495
E	2694	0.422

2.3 Methods

2.3.1 Tissue Preparation

All tissue preparation was performed by Dr. Selina Sohre, University of Mainz. The brains, which were stored at -80°C, were transferred to a sterile plastic dish and treated to thaw briefly at room temperature. The brains were divided into two hemispheres, and the right hemispheres were stored again at -80°C. The left hemispheres were transferred to a 10 cm cell culture dish with an ice-cold preparation of the Ringer solution. Then, the left hemispheres were divided into the areas of the cerebellum, the thalamus, the hippocampus, and the cortex. The tissue pieces were homogenized and sonicated in a non-denaturing lysis buffer at 4°C (Table 2). At the end, the samples were diluted for Western Blot analysis with denaturing lysis buffer. For each dilution (cerebellum 1:3, cortex 1:8, hippocampus 1:2, thalamus 1:3), a denaturing lysis buffer (Table 2) was adopted accordingly, so that all samples contained the same concentration of salts and detergents after the dilutions: 100 mM Tris, 0,5% SDS, 20% Saccharose, pH=7.4. All samples were stored at -80°C.

The current project, total extracts from the thalamus, the hippocampus, and the cerebellum were analyzed and studied.

2.3.2 Determination of Protein Concentration

The protein concentration in diluted samples was measured with the Bicinchoninic acid (BCA) assay kit by Thermo Fisher. The diluted samples were thawed on ice, vortexed, and briefly centrifuged. Meanwhile, BCA Working Reagent was prepared at a 50:1 ratio of Reagent A to Reagent B. The working reagent was mixed until it appeared homogeneous and had a light green color. A standard dilution series out of six dilutions was prepared during this time from a 2 mg/ml Biovine serum albumin (BSA) stock.

95 µl of the Working Reagent was mixed with 5 µl of the samples in standard 96-well plates, and the plates were incubated at 37°C for 30 minutes. After incubation, the plates were allowed to cool down to room temperature. Then, the absorbance of the solution was measured at 562 nm using a spectrophotometer. A standard curve of absorbance versus protein concentration was created using the absorbance readings of the standards. Then, the protein concentration was determined by comparing the absorbance of the unknown samples to the standard curve.

2.3.3 Sodium Dodecyl Sulfate-Polyacrylamide Gel Electrophoresis (SDS-PAGE)

During SDS-PAGE, proteins are separated according to their molecular weights. The samples were thawed in ice, vortexed and briefly centrifuged. 15 µl of each sample was added to 5 µl 4x loading buffer. Then, the mixtures were heated in a thermomixer at 95°C for 5 minutes and afterwards centrifuged for 5 seconds. For the SDS-PAGE, the Criterion Cell gel chamber with a suitable Criterion TGX precast gels were used. The gel was put into the chamber, and it then was filled with 1x running buffer. The comb was removed, and 15 µl of the previous mixture was added onto each lane of the gel. To assess protein molecular weights, 4 µl of PageRulerTM Prestained Protein Ladder was added to the first lane.

The top of the chamber was covered, the electrodes were connected, and the electrophoresis was run at 80 V for 10 min, and afterwards at 150 V for 50 min with a PowerPac HC High-current power supply. The SDS-PAGE was stopped when the downmost marker of the PageRulerTM Prestained Protein Ladder had almost reached the foot line of the glass plate.

2.3.4 Western Blot

After the SDS-PAGE was finished, the gel was taken out of the system. The components of the Western Blot sandwich were then equilibrated. Soaked with transfer buffer, a blotting sandwich was built from a sponge, blot absorbent paper, and above it the gel. On top of the gel, a cellulose membrane was added, then another blot absorbent paper, and lastly a sponge. After the second absorbent paper had been added, the sandwich was smoothed to expel air bubbles. The chamber of the Criterion Blotter was filled with 1x transfer buffer, which the sandwich was put into. It then was covered, the electrodes connected, and blotting was performed with the Criterion Blotter and PowerPac HC high-current power supply for 30 minutes at 100 V.

After the blotting, the membrane was taken out of the sandwich and stained with Ponceau solution for 10 minutes. Then, the stained membrane was washed with water until only the protein lanes were visible. A picture of the Ponceau staining was taken with an Amersham Imager 600, and the membrane was cut according to the visible lanes. To remove the Ponceau stain, the membrane was carefully washed three times for 5 minutes with TBS-T and then blocked for 1 h with 20 ml of blocking buffer. The blocking of the membrane is for the purpose of covering up all parts of the membrane that have protein on them, including any regions

between lanes, which prevents the non-specific binding of antibodies including both primary and secondary to the membrane in order to avoid high background in Western Blotting.

After that, the membrane was washed three times with TBS-T for 5 minutes, and the primary antibody was added and incubated overnight at 4°C. The following day, the membrane was washed three times with TBS-T, then the secondary antibody was added and incubated for 90 minutes at room temperature. After the incubation, the membrane was washed three times with TBS-T and a signal was detected. For this, ECL-solution A, ECL-solution B, and H_2O_2 were mixed at a 100:10:1 ratio, and 1.5 ml of this mixture were slowly added on top of the membrane. The chemiluminescent bands were made visible with an Amersham Imager.

Then, the membrane was washed with TBS-T. A β-tubulin primary antibody was added to the membrane and incubated over night at 4°C. The same steps were followed as before. The next day, the β-tubulin signal was detected, and a picture was taken. All antibodies and their data can be found in Table 4.

2.3.5 Data Evaluation

After detecting the signal, the intensity of the bands in each image was measured with AIDA Image Analysis software (AIDA ORGA GmbH).

The obtain values were divided by the intensity of the bands of ß-tubulin to normalize the amount of the protein of interest to the amount of total protein. The normalized values were also divided by the normalized values of total tau.

The resulting numerical data were evaluated with SigmaPlot software by one-way ANOVA, followed by Holm-Sidak Post-Hoc-test (software SigmaPlot 12.3). Thereby the groups that had been treated with MK-801 were compared to the control group. p-values ($p \leq 0.001$) shown in the figures were generated with the post-hoc-test. overall significances ANOVA significance levels are provided in the figure legend text. Other information, including the F-values and the degrees of freedom, are available in the Appendix "Statistical analysis". Each one-way ANOVA was always completed with an ANOVA on Ranks (Dunn´s Method), and this additional information is available in the Appendix “Statistical analysis.”

3. Results

3.1 Effect of Acute NMDA Receptor Inhibition in Male Wild-Type Mice in Vivo

To evaluate the hypothesis if decreased NMDA receptor function could contribute to the formation of Alzheimer's Disease typical histopathology such as tau tangles, 25 male wild-type mice an age of ten weeks (which did not overexpress any human genetic mutation), were allocated to five groups. The control group did receive saline, the other four groups were treated with one dose of the NMDA receptor antagonist MK-801 in saline and were then killed one, two, four or 24 hours after the treatment. Lysates from defined brain regions were prepared (3.3.1). For this study, lysates from the thalamus, the cerebellum, and the hippocampus were prepared and analyzed by Western Blot. An appropriate gel system with 25 lanes was used to analyze side by side the lysates prepared from 25 mice.

To detect the phosphorylation of tau protein, two antibodies were used (PHF1 and CP13). These non-commercial monoclonal antibodies were generously contributed by Dr. Peter Davies (Feinstein Institute for Medical Research, Manhasset, NY, USA). The PHF1 antibody detects phosphorylation of tau at two epitopes, Serine 396 (S396) and Serine 404 (S404) (Greenberg et al., 1992), whereas the CP13 antibody detects tau phosphorylation at the epitope Serine 202 (S202) (Petry et al., 2014; Xia et al., 2020). These epitopes are typically phosphorylated in Alzheimer´s disease, and both antibodies are widely used in Alzheimer´s disease research.

3.1.1 Analysis of Tau Phosphorylation in the Thalamus

The human thalamus is a complex of nuclei which is placed in the diencephalon and contains four parts (the hypothalamus, the epithalamus, the ventral thalamus, and the dorsal thalamus). The thalamus is a transmit center supporting both sensory and motor mechanisms, and thalami's nuclei (50–60 nuclei) project to a few well-defined cortical area (Herrero et al., 2002). Thalamic nuclei are functionally divided into three main groups: sensorimotor nuclei, limbic nuclei, and nuclei bridging these two zones (Vertes et al., 2015).

It has been shown that the thalamus is one of the regions in the brain which is affected by amyloid pathology and tau phosphorylation in Alzheimer´s disease. Braak´s model suggests that tau deposits begin in the thalamus in stage Ⅲ/Ⅳ (Braak and Braak 1991). The infliction of the thalamus may play a role in the development of attentional and memory-related problems in both early MCI and Alzheimer´s disease dementia (Van de Mortel et al. 2021).

Therefore, it was important in this study to examine the role of NMDA receptor on tau expression in the thalamus.

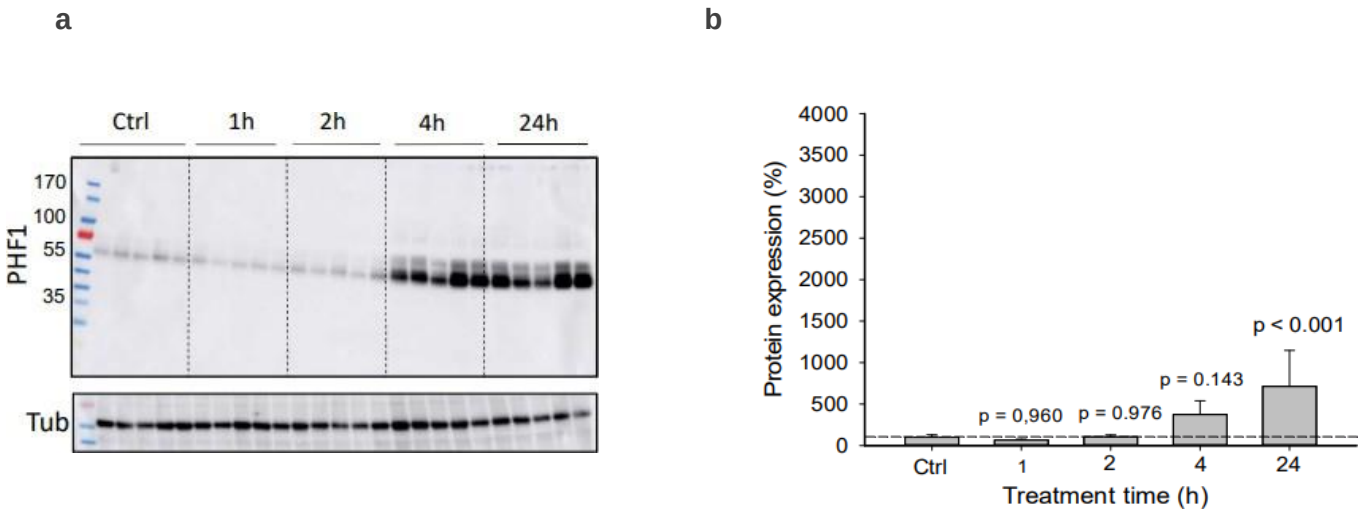

Figure 3: PHF1-tau phosphorylation in the thalamus.

Male wild-type mice were treated with a single dose of 5.0 mg/kg of MK-801 i.p. and killed 1, 2, 4, or 24 h later. Thalamus lysates were prepared, and tau phosphorylation was analyzed with the PHF1 antibody (a). An increase of the signal was detected at 55 kDa. Protein abundance was quantified and normalized to tubulin (b). Statistical significance between all groups was evaluated by one-way ANOVA (n = 5, p < 0.001). Statistical significance between each group (1h, 2h, 4h, or 24h) and the control group (vs. Ctrl) was evaluated by post-hoc test performed after the one-way ANOVA (the p-value for each group compared with the control group is provided in Figure 3b).

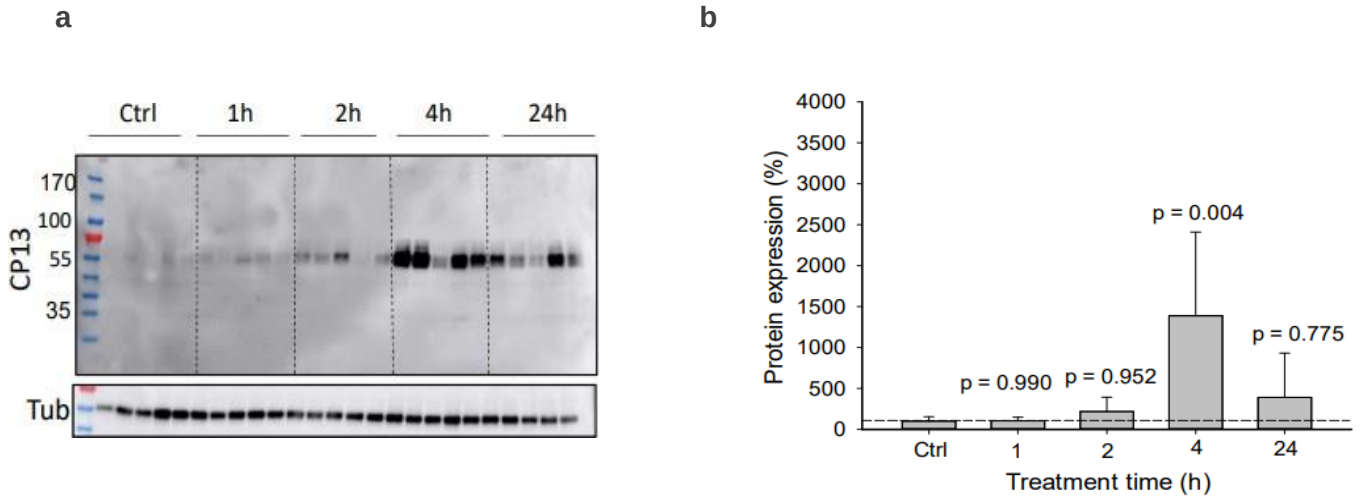

Figure 4: CP13-tau phosphorylation in the thalamus.

Male mice were handled with a single dose of 5.0 mg/kg of NMDA receptor blocker i.p. and killed 1, 2, 4, or 24 h later. The tissues were prepared, and tau phosphorylation was examined with the CP13 antibody (a). Protein intensity was quantified and normalized to tubulin (b). Statistical significance over all groups was studied by one-way ANOVA (n = 5, p = 0.004). Statistical significance between each group (1h, 2h, 4h, or 24h) and the control group (vs. Ctrl) was studied by post-hoc test (the p-value for each group is given in Figure 4b).

After the analysis of the thalamus tissue by Western Blot and generation of a membrane that included 25 lanes, the membrane was first treated with the PHF1 antibody. An image of the whole membrane is presented in Figure 3a. This figure displays the extent of tau phosphorylation in the thalamus of the investigated mice.

An increasing intensity of the bands was observed 4 hours and 24 hours after the injection of the NMDA-antagonist MK-801. Then, the same membrane was treated with an anti-tubulin antibody as loading control. The strength of the signal was approximately equal in all lanes.

To quantify the amount of tau phosphorylation, all bands were scored with image analysis, and the numerical results were statistically analyzed (Figure 3b). Figure 3b presents the percentile expression of tau phosphorylation in the thalamus in the control group and at various times after the injection of MK-801 (the dotted line in the figure denotes 100%). An increase in the extent of tau phosphorylation was observed in the 4 h and 24 h groups; the highest phosphorylation was measured after 24 hours. Tau phosphorylation in the 24 h group was about two times higher than in the 4 h group and eight times higher than in the control group. The 24 h group showed a significant increase ($p < 0.001$) compared to the control group.

The same thalamus lysates were used to prepare a new membrane by Western Blot, which was analyzed with the CP13 antibody (Figure 4a). A signal was obtained at 55 kDa, and a rise in strength of the signal was noticed 4 h and 24 h after the injection. The same membrane was treated with an anti-tubulin antibody. An image of the membrane after investigation for tubulin is also exhibited in Figure 4a.

The bands were quantified, normalized to tubulin, and then statistically analyzed (Figure 4b). The first expansion phosphorylation of tau was detected two hours after the treatment. The amount of tau phosphorylation was measured to 200%. The biggest difference was measured between the control group and the 4 h group, with an increase in phosphorylated tau of 1400%. After 24 h of the treatment, the increase in tau phosphorylation was quantified to be approximately 400%.

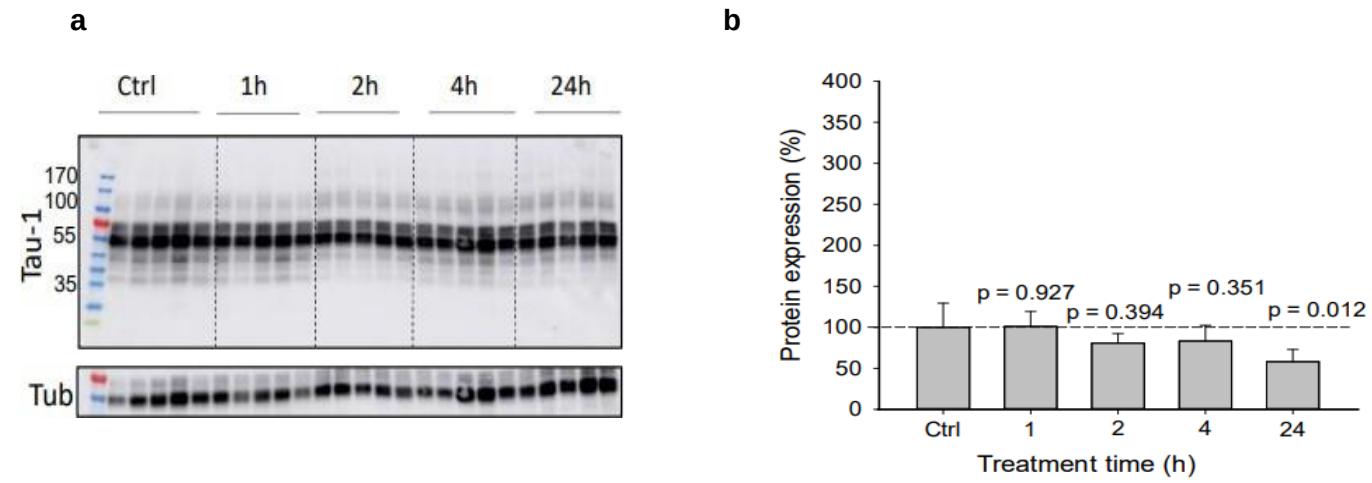

Figure 5: Total tau expression in the thalamus.

After receiving a single injection of MK-801 at a dose of 5.0 mg/kg, male mice were killed 1, 2, 24 hours later. Thalamic lysates were analyzed with the Tau-1 antibody (a). Tau protein expression was measured and adjusted to tubulin (b). A one-way ANOVA was used to assess the statistical significance between all groups (n = 5, p = 0.015), followed by post-hoc test to assess the statistical significance between each group individually (1 h, 2 h, 4 h, or 24 h) versus the control group (vs. Ctrl). In Figure 5b, the p-value for each group is displayed.

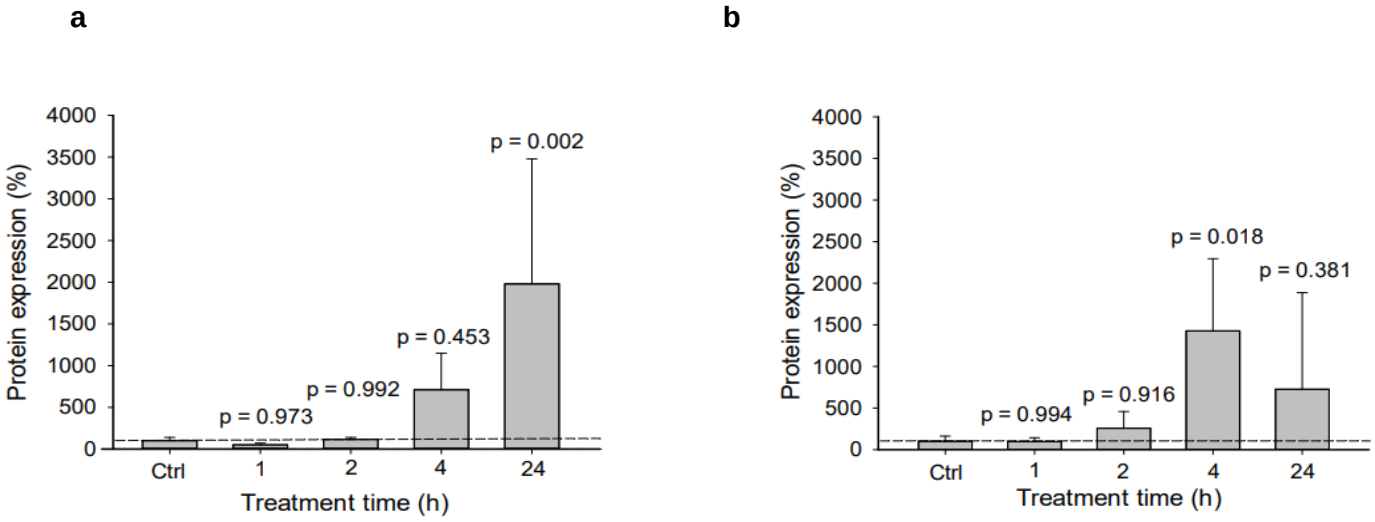

Figure 6: Quantification of tau phosphorylation in the thalamus of mice normalized to Tau-1.

Tau phosphorylation in the thalamus was normalized to Tau-1 after analysis by PHF1 antibody (6a) and CP13 antibody (6b). The statistical significance between all groups was evaluated by one-way ANOVA. 6a: PHF1 (n = 5, p < 0.001). 6b: CP13 (n = 5, p = 0.020). Statistical significance between each group (1 h, 2 h, 4 h, or 24 h) and the control group (vs. Ctrl) was evaluated by post-hoc test and the p-value for each group is shown in Figures 6a (after treatment with PHF1) and 6b (after treatment with CP13).

To examine if the apparent hyperphosphorylation of tau in the thalamus was indeed due to an increased relative phosphorylation of the epitopes (S404, S396, and S202), that are detected by PHF1 and CP13 antibodies or was due to an increase in total tau protein expression, the numerical values Figure 3b and 4b were normalized to total tau protein expression. Therefore, the same thalamus tissues were analyzed by Western Blot and examined with the Tau-1 antibody followed by anti-tubulin antibody (Figure 5a). The expression of total tau was stable and consistent between all groups (Figure 5a). The intensity of the bands was measured, standardized to tubulin, and statistically analyzed (Figure 5b). A modest decrease in the expression of tau protein was realized in the 24 h group. Next, the measured phospho-tau expression in the thalamus as per evaluation with PHF1 (Figure 3b) and CP13 (Figure 4b), which had already been normalized to tubulin, was additionally corrected for total tau, and the numerical data were statistically analyzed by one-way ANOVA (Figure 6).

Figure 6a represents the phosphorylation of tau after investigation with PHF1, normalized to total tau. In comparison to plain normalization to tubulin, the data were only slightly altered. An increase in tau phosphorylation was also observed 4 hours and 24 hours after the treatment. However, the numerical difference in tau phosphorylation between the 4 h group and the control group, as well as between the 24 h group and the control group, was greater than the difference when the bands had been normalized only to tubulin (Figure 3b).

The normalization of CP13-tau phosphorylation in the thalamus to total tau revealed a similar tendency (Figure 6b). The first rise in tau phosphorylation was identified 2 h after the injection, and the highest amount of tau phosphorylation was also calculated for the 4 group; the quantified tau phosphorylation in this group was approximately 15 times higher than tau phosphorylation in the control group.

In conclusion, the normalization of tau expression after treatment with PHF1 and CP13 to total tau in the thalamus did not substantially influence the data and showed an increase in tau phosphorylation compared to the control group. Therefore, it is reasonable to conclude that the determined results are due to increase in tau phosphorylation at the epitopes of PHF1 (S396, S404) and the epitope of CP13 (S202), and not caused by increased expression of the total tau protein.

3.1.2 Analysis of Tau Phosphorylation in the Hippocampus

The hippocampus is an expansion of the temporal part of the cerebral cortex. It can be observed as a layer of thickly packed neurons that forms an S-shaped structure on the edge of the temporal lobe (Dhikav and Anand, 2012; Gilbert and Brushfield 2009). The hippocampus is split into the hippocampus proper (cornu ammonis, CA), the dentate gyrus (DG), the

subiculum (SUB), and the entorhinal area (EC). Based upon histology, the hippocampus proper (CA) is subdivided into CA1, CA2, CA3, and CA4 (Figure 7) (Anand and Dhikav, 2012). The hippocampus is an important component of the limbic system (McDonald and Mott, 2017). It plays a key role in learning and memory (Lisman et al., 2017), spatial navigation (Stella et al., 2011) and emotional behavior (Toyoda et al., 2011).

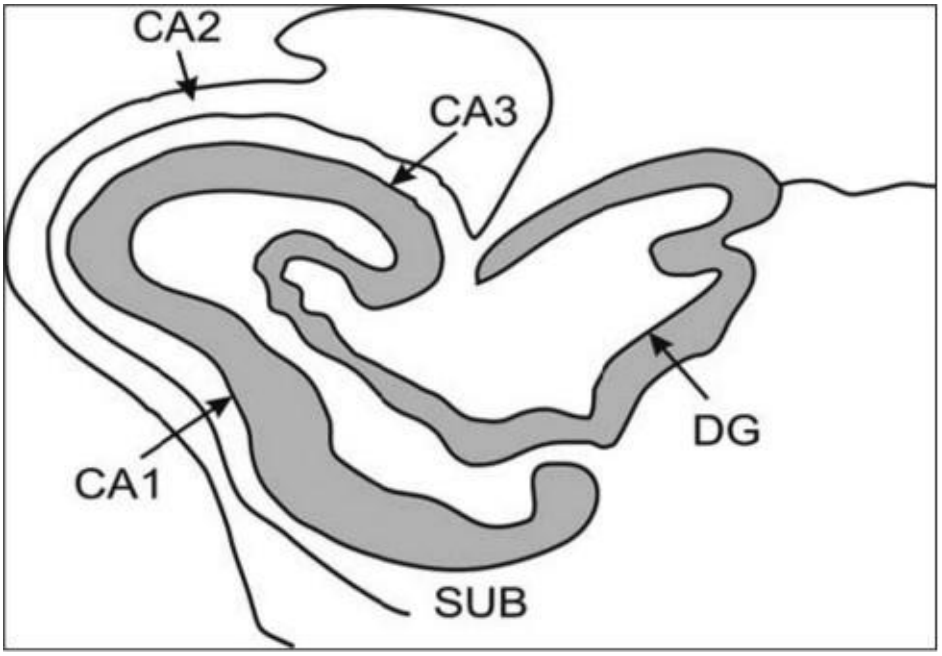

Figure 7: Microstructure of hippocampus.

The human hippocampus is a C-shaped structure that has been divided into distinct histological domains.CA: hippocampus proper, DG: dentate gyrus, SUB: subiculum (Anand and Dhikav, 2012).

The hippocampus is one of the earliest regions in the brain that is affected by neuropathological changes in Alzheimer´s disease. Generally, the entorhinal cortex is the first area in the medial temporal lobe to experience neuropathology, followed by the hippocampus (Braak et al., 1996). Besides, hippocampal atrophy was observed in patients with Alzheimer´s disease. It has been realized that patients with Alzheimer´s disease exhibit 15-30% loss of the volume of the hippocampus (Frisoni et al., 2010). Furthermore, postmortem examination of the brains of patients with Alzheimer´s disease has revealed a reduced number of synapses in the CA1 region of the hippocampus and dentate gyrus (Scheff and Price 1998). Moreover, NMDA receptors are highly expressed in the hippocampus and play a significant role in memory

formation (Niewiadomska et al., 2009). For these reasons, it was essential to study the phosphorylation of tau in the hippocampus after NMDA receptor inhibition.

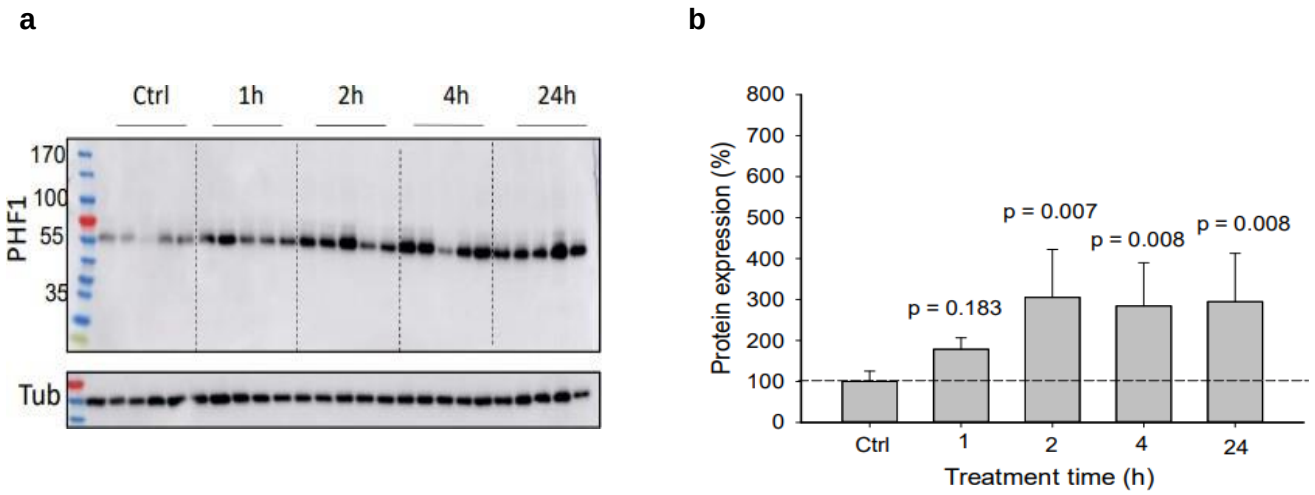

Figure 8: PHF1-tau phosphorylation in the hippocampus.

Male mice were given a single dose 5.0 mg/kg of MK-801 i.p. and analyzed 1, 2, 4, or 24 h later. The hippocampus was prepared, and tau phosphorylation was analyzed with the PHF1 antibody (a). The intensity of the signal was quantified and adjusted to tubulin (b). One-way ANOVA was used to determine statistical significance between all groups (n = 5, p = 0.006), the Holm-Sidak post-hoc test was conducted to assess the differences between each individual group (1h, 2h, 4h, or 24h) versus the control group (vs Ctrl). In Figure 8b, the p-value for each group is presented.

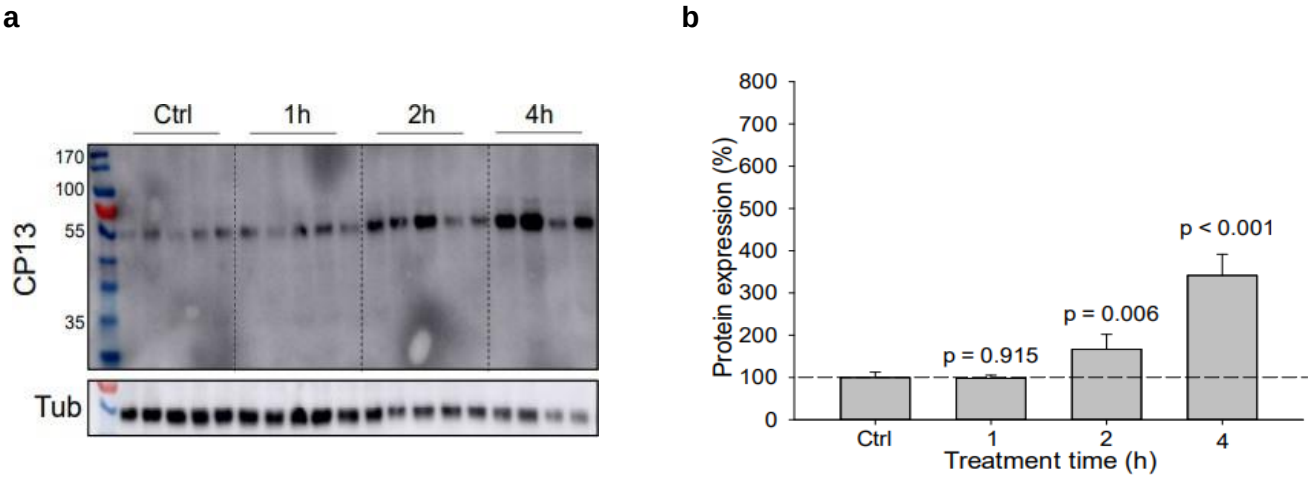

Figure 9: CP13-tau phosphorylation in the hippocampus.

Male mice were analyzed 1, 2, or 4 hours after receiving a single dose of 5.0 mg/kg of MK-801 i.p. Tau phosphorylation was studied with the CP13 antibody (a). Protein abundance was quantified and normalized to tubulin (b). Statistical significance between all groups was studied by one-way ANOVA (n = 4, p < 0.001). Statistical significance between each group 1h, 2h, or 4h versus the control group (vs. Ctrl) was determined by post-hoc test. The p-value for each group is provided in Figure 9b

The 25 hippocampus tissues were studied by Western Blot (like in the thalamus). They were first analyzed with the PHF1 antibody (Figure 8a). A growth signal intensity was found one hour after the injection.

The strength of the bands at 55 kDa were measured with AIDA and normalized to tubulin (Figure 8b). The rise in tau phosphorylation after one hour 180%, phosphorylation continued to expand to reach 300% two hours after the treatment and was almost steady at 300% in 4 hour group and 24 hour group.

After examination with the PHF1 antibody, the hippocampus lysates were analyzed with the CP13 antibody (Figure 9a). Only four groups are shown in the figure, because a lack of material precluded the assessment of the 24 hour group. Quantitative analysis of the intensity of the bands and normalization to tubulin is presented (Figure 9b), the fifth band of the 4 hour group had to be excluded from the quantification for technical error. The first increase in tau phosphorylation was observed 2 hours after the injection. However, the highest amount of tau phosphorylation in comparison to the control group was measured in the 4 hour group (300%). The 4 hour group revealed a significant increase compared to the control group ($p < 0.001$).

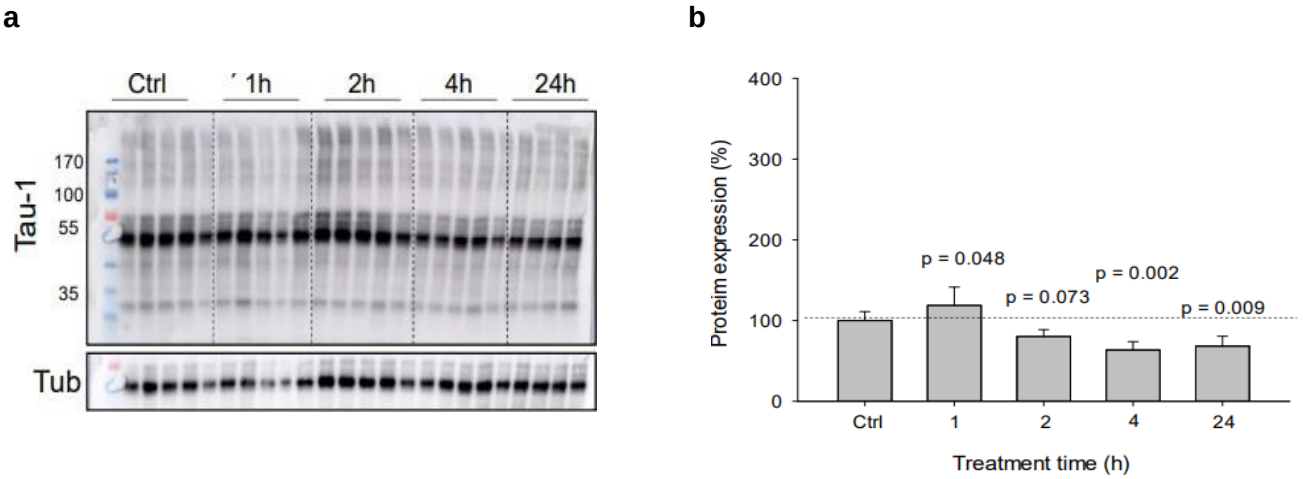

Figure 10: Total tau expression in the hippocampus.

The Tau-1 antibody was used to determine the expression of total tau in the hippocampus of 25 male mice after injection of 5.0 mg/kg of MK-801 (a). The strength of protein expression was measured with AIDA and to tubulin (b). A one-way ANOVA, followed by post-hoc test was used to study the statistical significance between all groups ($n = 5$, $p < 0.001$), and between each group individually (1 h, 2 h, 4 h, or 24 h) versus the control group (vs. Ctrl). The p-value for each group is shown in Figure 10b.

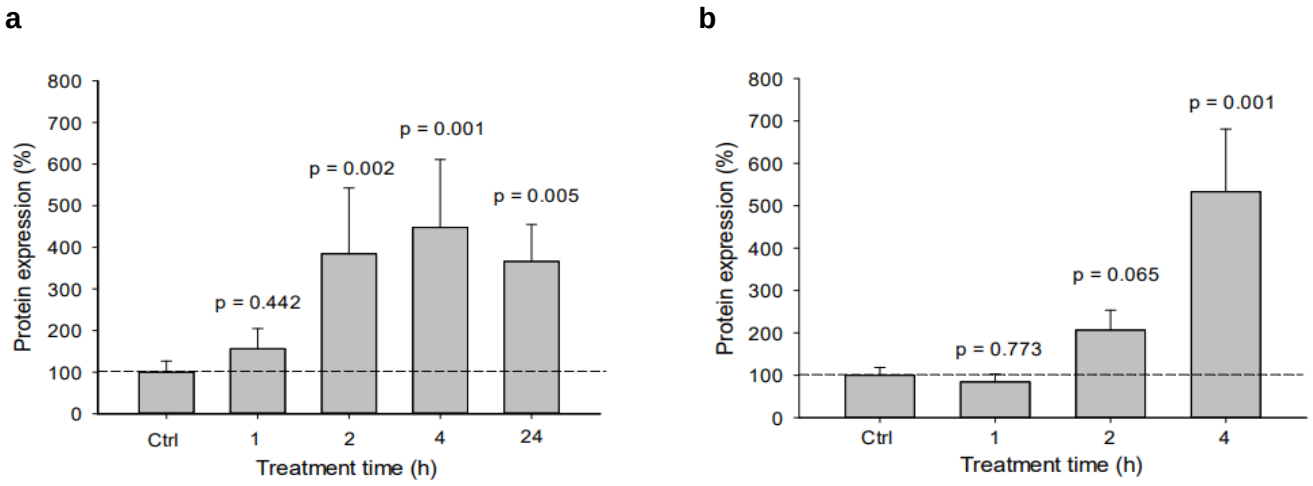

Figure 11: Quantification of tau phosphorylation in the hippocampus of mice normalized to Tau-1.

Tau phosphorylation in the hippocampus was standardized to total tau expression after treatment with a single dose of 5 mg/kg MK-801 and analysis by PHF1 antibody 11a and CP13 antibody 11b. A one-way ANOVA was used to determine the statistical significance between all groups. 11a: PHF1 ($n = 5$, $p < 0.001$); 11b: CP13 ($n = 4$, $p < 0.001$). The statistical significance between each group (1 h, 2 h, 4 h, or 24 h) versus the control group (vs. Ctrl) was determined by Holm-Sidak post-hoc test. The p-value for each group is given in Figures 11a (after treatment with PHF1) and 11b (after treatment with CP13).

Next, the expression of total tau was investigated in the hippocampus using the Tau-1 antibody, and the expression was evaluated statistically (Figure 10). Only 24 bands are shown (Figure 10a), as a lack of material precluded the analysis of the fifth mouse in the 24 hour group.

PHF1-tau phosphorylation and CP13-tau phosphorylation in the hippocampus were also normalized to total tau (Figure 11). The normalization to total tau displayed similar results as the normalization to tubulin. A non-significant increase in PHF1-tau phosphorylation was realized in the first hour after the treatment, and the highest tau phosphorylation was measured in the 2 h and the 4 h groups (Figure 11a). An increase in CP13-tau phosphorylation was detected 2h and 4h after the injection (Figure 11b), with the largest increase in tau phosphorylation in the 4 h group.

3.1.3 Analysis of Tau Phosphorylation in the Cerebellum

For a long time, it was believed that the cerebellum was only responsible for the coordination of voluntary motor activity and motor learning (Jacobs et al., 2018). Thus, the role of the cerebellum in Alzheimer´s disease has not received much attention either, and some

Alzheimer´s disease studies have indeed used the cerebellum as a reference region (Smith et al., 1997). However, it has been demonstrated more recently that the cerebellum provides non-motor function-related cognitive, behavioral, and affective processing (Singh-Bains et al., 2019). Furthermore, the cerebellar cognitive-affective syndrome (CCAS), which is represented by the presence of cerebellar lesions, exhibits hallmark deficits in executive function, linguistic processing, visuospatial cognition, and emotional modulation (Schmahmann and Sherman, 1998; Schmahmann, 2004). These data support that modifications in the cerebellum do not only affect motor functions, but also cognitive and affective functions.

Pathological changes within the cerebellum have been reported in Alzheimer´s disease, for example cerebellar amyloid-β deposits within the molecular, granular and Purkinje cell layers of the cerebellar cortex, a loss of Purkinje cells in the Alzheimer´s disease cerebellum compared to control brains, and cerebellar atrophy (Jacobs et al., 2018).

Therefore, after studying of the expression of tau phosphorylation in the thalamus and the hippocampus of the MK-801 treated mice, it was interesting to investigate the tau phosphorylation in the cerebellum of these mice.

a **b**

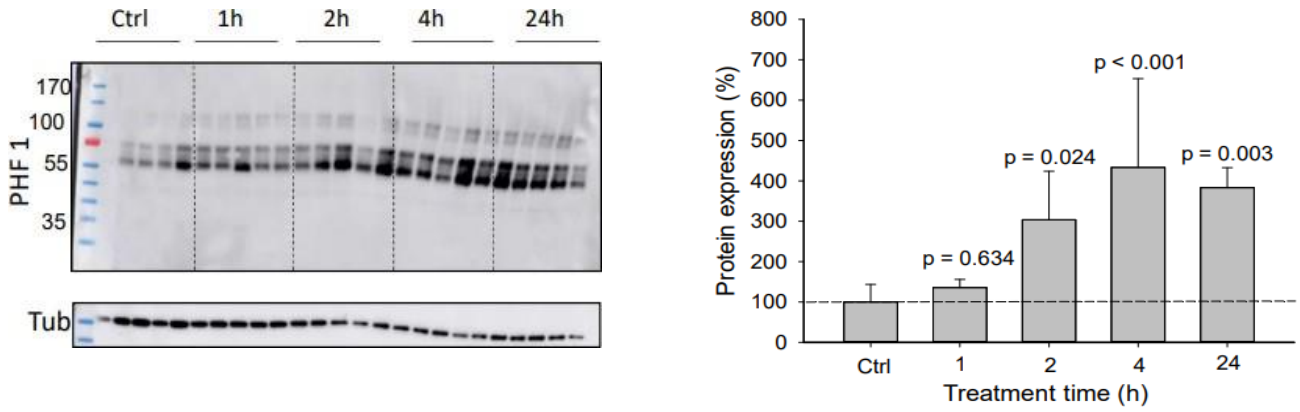

Figure 12: PHF1-tau phosphorylation in the cerebellum.

Lysates were prepared from the cerebellum of MK-801 treated mice at separate times (1 h, 2 h, 4 h, 24 h) after the injection, and the PHF1 antibody was used to detect tau phosphorylation (a). The expression of the signal was quantified and normalized to tubulin (b). Statistical significance across all groups was evaluated by one-way ANOVA (n = 5, p = 0.004). Statistical significance between each group (1 h, 2 h, 4 h, or 24 h) versus the control group (vs. Ctrl) was examined by post-hoc test. The p-value for each group is given in Figure 12b.

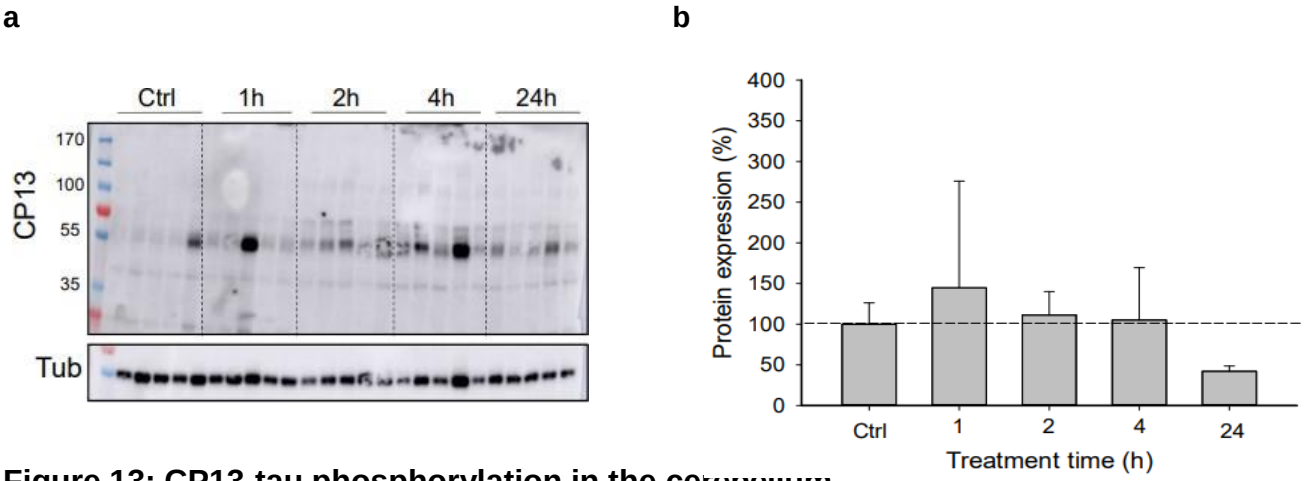

Figure 13: CP13-tau phosphorylation in the cerebellum.

Lysates were prepared from the cerebellum of MK-801 treated mice at various times (1 h, 2 h, 4 h, 24 h) after the injection, and the CP13 antibody was used to study tau phosphorylation (a). The strength of the signal was measured with AIDA and normalized to tubulin (b). Statistical significance between all groups was evaluated by one-way ANOVA (n = 5, p = 0.295,). The differences in the mean values across the treatment groups were not statistically significant.

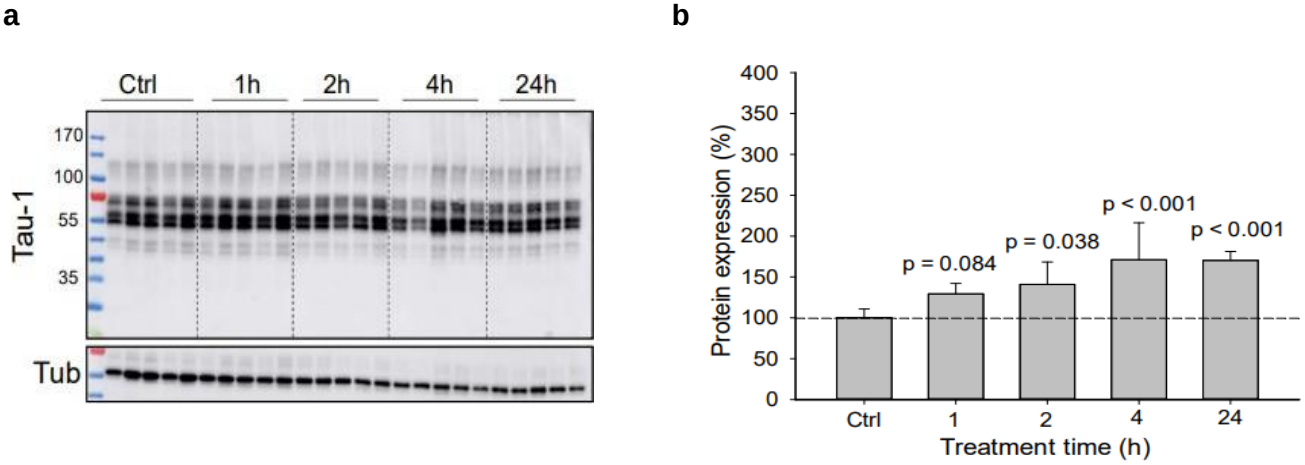

Figure 14: Total tau expression in the cerebellum.

The expression of total tau in the cerebellum was assessed using the Tau-1 antibody (a). The strength of the signal was measured with AIDA and normalized to tubulin (b). A one-way ANOVA, followed by Holm-Sidak post-hoc test, was used to analyze the statistical significance across all groups (n = 5, p = 0.017) and between each group individually (1 h, 2 h, 4 h, or 24 h) versus the control group (vs. Ctrl). The p-value for each group is given in Figure 14b.

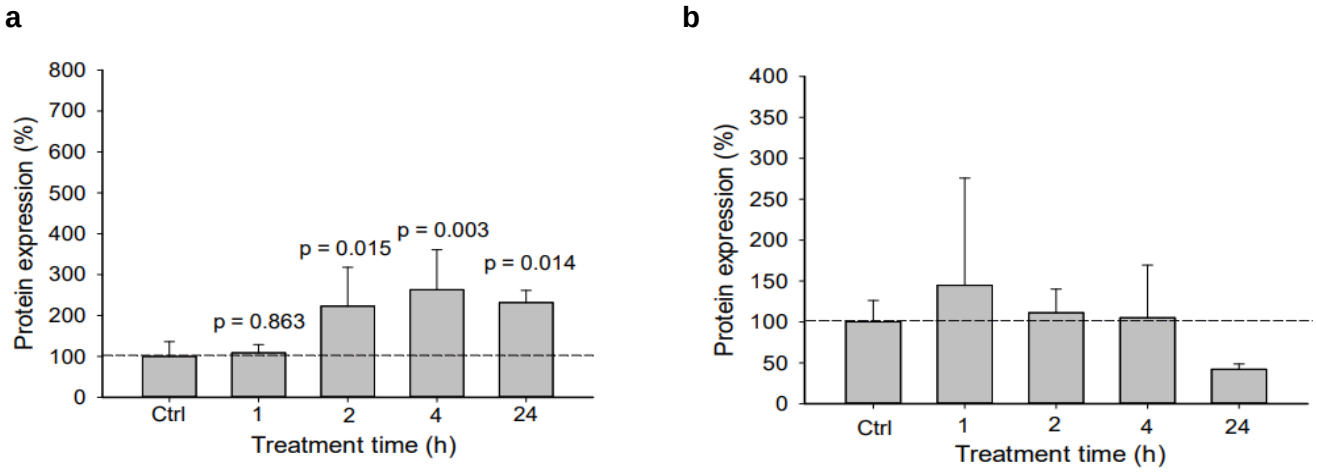

Figure 15: Quantification of tau phosphorylation in the cerebellum of mice normalized to Tau-1.

Tau phosphorylation in the cerebellum was adjusted to total tau after analysis with the PHF1 antibody (15a) and the CP13 antibody (15b). Using a one-way ANOVA, the statistical significance between all groups was assessed. 10a: PHF1 (n = 5, p 0.001). 10b: CP13 (n = 5, p = 0.240). A post-hoc test was used to assess the statistical significance between each group individually (1 h, 2 h, 4 h, or 24 h) versus the control group (vs. Ctrl). Figure 15a (after administration of PHF1) displays the p-values for each group. Figure 15b, no post hoc test p-values could be calculated due to the lack of significance in the ANOVA.

Analysis of the cerebellum with the PHF1 antibody demonstrated bands at 55 and 70 kDa (Figure 12a). There was a visible increase in tau phosphorylation after the treatment with MK801. Interestingly, the tau signal of PHF1 in the cerebellum was divided into two distinct bands with variable intensity, hence different isoforms might have been detected here. The intensity of the bands was measured, and the resulting data was normalized to tubulin and then statistically analyzed (Figure 12b). The first increase in tau phosphorylation was realized 2 h after the treatment, but the highest increase was recognized after 4 h and was estimated at 400%. The 4 h groups and the 24 h groups exhibited a statistically significant increase in tau phosphorylation compared to the control group.

Next, the cerebellum was analyzed with the CP13 antibody (Figure 13a). No significant systematic rise in the signal of the bands was observed in any group. An apparently unsystematic signal increase was realized selectively in the third mouse of the 1 hour group, and in the fourth mouse in the 4 hour group. After quantification of the bands and normalization to tubulin, the numerical results were analyzed with one-way ANOVA (Figure 13b). There were

no statistically significant differences between the groups. The p value over all groups was p = 0.295, and therefore, the ANOVA software did not calculate any p-values between each treated group and the control group.

The data were also normalized to total tau expression. The examination of the cerebellum lysates with the Tau-1 antibody (Figure 14a) and a statistical analysis of the resulting data after normalisation to tubulin (Figure 14b). The data in Figure 14 indicate a modest, but suignificant induction of total tau expression relative to Tubulidentata after MK-801 Treatment in the cerebellum. The increase in PHF1-tau phosphorylation in the cerebellum was partially attenuated by normalization to total tau (Figure 15a). An increase in phosphorylation was still seen 2, 4, and 24 hours after the injection, and the highest protein expression was measured after 4 hours. The data from the analysis of the cerebellum with the CP13 antibody was also normalized to total tau (Figure 15b), but no significant differences between the groups were realized with a p value over all groups of p=0.240.

In conclusion, only the PHF1 antibody detected an increase in tau phosphorylation in the cerebellum after blocking NMDA receptor with MK-801 in vivo, whereas the analysis with the CP13 antibody did not show any systematic increase with or without correction for baseline tau expression.

3.2 Cross-Comparison of Tau Phosphorylation in Different Brain Regions of the Control Group Mice

In this expirement, the increase in tau phosphorylation in each area of the brain of the MK-801-treated mice should be compared to the extent of tau phosphorylation in the same area of the brain of the mice control group.

Therefore, four areas of the brain (the cortex, the hippocampus, the thalamus, and the cerebellum) of thecontrol group were analyzed by Western Blot with the PHF1 and CP13 antibodies, normalized to tubulin, and statistically analyzed. The results are shown in Figures 16 and 17.

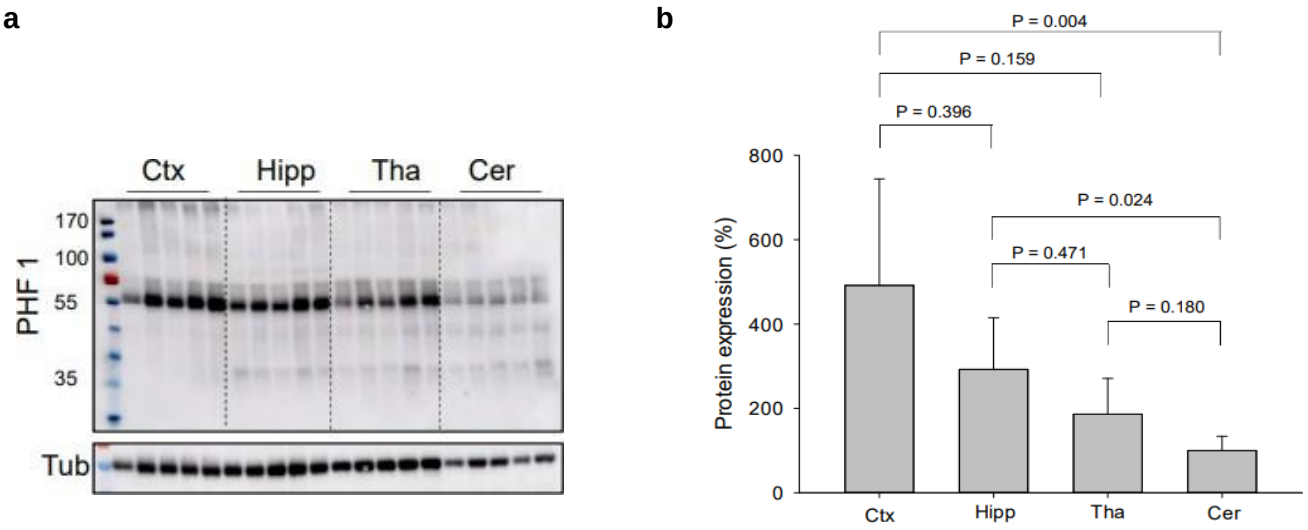

Figure 16: PHF1-tau phosphorylation in different areas of the brain.

Figure 16a presents the extent of tau phosphorylation in different regions (the cortex (Ctx), the hippocampus (Hipp), the thalamus (Tha), and the cerebellum (Cer)) of the brain of the control mice (not treated with MK-801) after analyzing them with the PHF1 antibody. The intensity of the bands was measured with AIDA, normalized to tubulin (16b), and statistically evaluated by one-way ANOVA (n = 4, $P < 0.001$). All pairwise multiple comparison p-values between each two areas are provided in the graph.

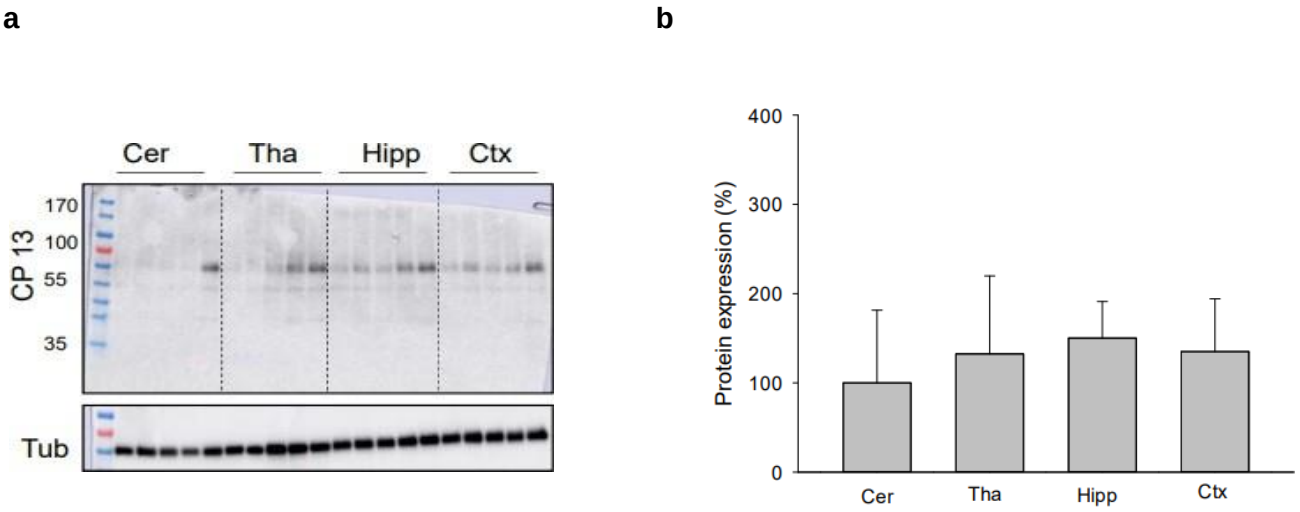

Figure 17: CP13-tau phosphorylation in different areas of the brain.

Different areas of the brains of the control group of mice (the cerebellum, the thalamus, the hippocampus, and the cortex) were studied with the CP13 antibodies (Figure 17a). The signal quantified, evaluated with AIDA, normalized to tubulin, and statistically analyzed by one-way ANOVA (n = 4, p = 0.629) (17b). Abbreviations are used in Figure 16b.

The analysis of the control group mice with the PHF1 antibody exhibited different degrees of baseline tau phosphorylation in the different brain areas (Figure 16a). The highest baseline phospho tau was observed in the cortex and the lowest in the cerebellum. The intensity of the bands was measured with AIDA, normalized to tubulin, and statistically analyzed (Figure 17b). The amount of tubulin in the cerebellum was less than the amount of tubulin in other regions of the brain. The highest amount of Tubulin-normalized tau phosphorylation was measured in the cortex (approximately two and a half times more than in the cerebellum). The second highest phosphorylation of tau was exhibited by the hippocampus, followed by the thalamus. The cerebellum presented the lowest measured relative level of tau phosphorylation.

The mice in the control group were also studied with the CP13 antibody. No systematic difference was observed between the different areas of the brains of these mice, but a certain variability in tau phosphorylation was observed between the mice of each group. For example, in the cerebellum, the fifth mouse showed an apparently higher level of tau phosphorylation than the other mice. However, the same variability had been detected before (Figures 3, 8, 13), validating the Western Blot methodology even at the apparently low expression levels of the CP13 epitope in control mice. After analysis with one-way ANOVA, the variation in tau phosphorylation between the different regions was not larg enough to exclude randomness ($p = 0,629$). Therefore, all-pairwise p-values between each two areas could not be calculated.

4. Discussion

4.1 Effect of NMDA Receptor Blockade on Tau Phosphorylation

In the present study, an increase in tau phosphorylation following the blockade of glumatergic neurotransmission via NMDA receptor with the chemical MK-801 was observed in different areas of the brain of male mice. The quantitative increase in tau phosphorylation was in part substantial and similar to the increase in tau phosphorylation in pathological situations, and it was also observed to be dynamic and tissue specific, as the amount of phosphorylated tau was variable in different areas of the brain.

In the literature, a reciprocal connection between tau and NMDA receptor activity has already been described several years ago: phosphorylated tau interacts with the kinase Fyn, which in turn phosphorylates the NR subunit 2 (NR2) of the NMDA receptor, which promotes the interaction of the receptor with the postsynaptic density protein 95 (PSD-95). As a result, NRs link to excitotoxic downstream signaling (Ittner et al., 2010). Accordingly, a deletion of tau in transgenic mice interrupted the postsynaptic targeting of Fyn, reducing the interaction of NRs with PSD-95 and protecting mice from NMDA receptor mediated excitotoxicity and memory deficits (Ittner et al., 2010; Roberson et al., 2007). Additionally, overexpressing tau resulted in hyperexitability (Maeda et al., 2016). It was also demonstrated that the tau protein plays a role in motor and cognitive functions, and an acute knockout of tau in the hippocampus was reported to impair cognitive performance (Velazquez et al., 2018).

Another study has shown that NR2B subunits, which also form NMDA receptor with NR1 subunits, are transported along microtubules by the kinesin superfamily motor protein KIF 17 (Setou et al.,2000). Notably, tau protein is a microtubule-binding protein and plays a role in the regulation of kinesin and dynein motor proteins (Dixit et al., 2008). These results refer to a possible role of tau protein in the regulation of NR2B protein transport. To remember, in Alzheimer´s Disease (Alzheimer´s disease), the phosphorylation of the protein tau is the first step towards its aggregation and the formation of intracellular NFTs, one important hallmark of Alzheimer´s disease (Selkoe, 2013).

Besides Alzheimer´s disease, increases in tau phosphorylation occur frequently in pathological events such as mechanical damage (Edwards et al., 2017; Zanier et al., 2018) and under various interesting physiological phenomena such as hibernation (Arendt et al., 2003). The trigger of tau phosphorylation in these cases is still unclear. Some studies have suggested that disinhibition of excitatory neurotransmission via a complex neuroanatomical cascade was a possible trigger of hyperphosphorylation of tau in certain cortical areas (Wozniack et al., 1998;

Olney et al., 1997). These studies proposed that the blocking of NMDA glutamate receptors on GABAergic interneurons (GABA: gamma aminobutyric acid) leads to a decapacitation of glutamate as driver of GABAergic inhibitory interneuron activity, and as a result, a loss of inhibitory control over the cholinergic and glutamatergic excitatory projections upstream to the cerebral cortex. Finally, the muscarinic receptor system and non-NMDA glutamate receptor system in PC/RSC (posterior cingulate/retrosplenial cortex) the neurons and other cortical areas would become hyperactive, and second messenger pathways that are associated with these receptors would lead to hyperphosphorylation of the microtubule-associated protein tau.

In summary, a two-way regulatory interaction between the tau protein and NMDA receptors appears to exist, which might indeed represent a regulatory circuit, as further detailed below. In Alzheimer´s disease, NMDA receptors insufficiency could thus represent a common molecular trigger of learning and memory deficits on the one hand, and of tau phosphorylation towards pathological Alzheimer´s disease on the other hand.

4.2 The NMDA Antagonist MK-801

The NMDA receptor is involved in many different diseases, including neurodegenerative, neurodevelopmental, and mood disorders. However, because of the severe psychotic side effects of NMDA receptor blockers, the development of many of these drugs was stopped. Regardless, some uncompetitive NMDA receptor blockers were developed and reached the market stage like dextromethorphan, ketamine, esketamine (the S-enantiomer of ketamine), memantine, and amantadine (Ahmed et al., 2020) and usually possess more severe side-effects due to their pronounced inhibition at low agonist concentrations. Competitive antagonists compete directly against glutamate for binding to the NMDA receptor. This class of drug contains 2-amino-7-phosphono-hepatonate (APH), 4-(3-phosphonopropyl)-2-piperazinecarboxylic acid (CCP), andcis-4-phosphono-methyl-2-piperidine-carboxylic acid (Selfotel). Non-competitive antagonists do not bind at the glutamate site but rather work at the phencyclidine (PCP) site, hindering ionic current through the agonist activated channel; non-competitive antagonists, besides PCP, are ketamine, benzomorphans, dextrophan, dextromethorphan, and MK-801, which was used in this study (Madden 2002).

MK-801 ((+)-5-methyl-10,11-dihydro-5H-dibenzo[a,d] cyclohepten-5,10-imine), also known as dizocilpine, was shown to be a potent anticonvulsant agent with anxiolytic and sympathomimetic properties (Hucker et al., 1983); later, it was discovered that MK-801 is a potent antagonist of NMDA receptor (Wong et al., 1986). MK-801 is a non-competitive antagonist of NMDA receptor and shows a high degree of use-dependency (Woodruff et al., 1987). MK-801 binds inside the ion channel of NMDA receptor at PCP binding sites, preventing

the flow of ions, including calcium (Ca^{2+}); MK-801 requires depolarization of the neuron and opening the ion channel to bind inside the ion channel; thus, MK-801 blocks NMDA receptor in a voltage-dependent manner and belongs to the drug class of the “open-channel blockers” (Kovacic and Somanathan 2010).

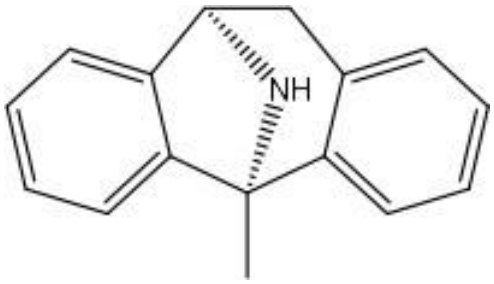

Figure 18: Chemical structure of MK-801.

MK-801 induced in rats a behavior syndrome with increased locomotion, stereotypies, and ataxia (Andiné et al., 1999). It also induced, like other NMDA receptor antagonists, amnesia and impairment of learning and memory in a variety of tasks in rats, mice, and other species (Kovacic and Somanathan 2010). Besides, it has been shown that the treatment of rats with high-dose MK-801 triggered neuronal degenerations in different regions of the brain (Wozniak et al., 1998; Horváth et al., 1997).

The half-life of MK-801 in rats was reported to be around 2 hours (Vezzani et al., 1989); the high dose of MK-801 that has been used in this study is close to concentration (10mg/kg) that has been shown to cause selective, irreversible degeneration of a small number of PC/RSC neurons, including that it might represent the highest applicable dose that can be used without causing permanent structural damage (Newcomer, Farber, and olney 2000; Allen and Iversen 1990).

4.3 Detecting the Phosphorylation of Tau at Specific Epitopes

The longest form of human tau contains 441 amino acids. In Alzheimer´s disease, tau can be phosphorylated at a minimum of 19 specific amino acid sequences (Figure 19). The formation of neurofibrillary tangles (NFTs) happens in several steps; it was observed that there are three different morphological stages of NFTs: pre-NFT, intra-neuronal, and extra-neuronal NFT

(iNFT and eNFT). These NFTs show in each stage a different phosphorylation at specific epitopes (Augustinack et al., 2002; Kimura et al., 1996).

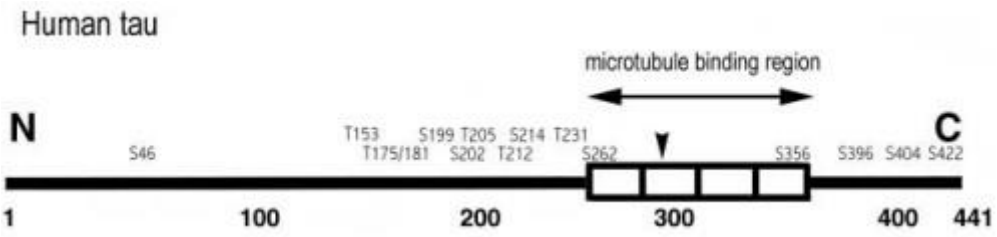

Figure 19: Human Tau.

The full-length form of human tau has 441 amino acids. The phosphorylation sites or epitopes are labeled in the upper half of the figure (S serine, T threonine, white rectangle homologous repeat, *N* terminal, *C* terminal) (Augustinack et al., 2002).

In this study, two antibodies (PHF1 and CP13) were used to analyze the phosphorylation status of tau protein; both antibodies were a generous gift from Dr. Peter Davies (Albert Einstein College of Medicine, NY, USA).

The PHF1 antibody is directed against a doubly phosphorylated epitope, serine 396 (S396) and serine 404 (S404) (Greenberg et al., 1992; Lang et al., 1992). This antibody stained mainly eNFT and NTs and, to a lesser degree iNFT; this means that iNFT and eNFT are both phosphorylated at the S396 and S404 epitopes (Augustinack et al., 2002).
Different kinases contribute to the phosphorylation of tau protein at S396 and S404; glycogen synthase kinase 3ß (GSK-3ß) phosphorylates tau mainly at S404 and S396. Mitogen-activated protein kinase (MAPK) also phosphorylates tau at both of these epitopes, but it shows its highest activity at other epitopes like serine 235 and threonine 153. Other kinases, like cyclin-dependent kinase 5 (cdk5) and cyclin-dependent kinase 2 (cdk2), phosphorylate tau at the S404 epitope but not at the S396 epitope (Illenberger et al., 1998).

The second antibody used in this study (CP13) detects tau phosphorylation at the epitope serine 202 (S202) (Xia et al., 2020). S202 is also phosphorylated by different kinases; cdk5 and cdk2 show high phosphorylation activity at S202; otherwise, MAPK and GSK-3ß phosphorylate tau weakly at S202 (Illenberger et al., 1998).

One of the kinases mentioned above (GSK-3ß) was already reported to be induced by NMDA receptor antagonism, which strengthens the hypothesis of this study (Lei et al., 2008).

4.4 Tau Phosphorylation in Different Areas of the Brain

The different areas of the brain exhibited different extents of tau phosphorylation after injection of MK-801 and analysis with different antibodies. The control group mice, which were not treated with NMDA receptor blocker, also showed a differential baseline tau phosphorylation in the different areas of the brain (Figures 15, 16). Therefore, the numerical results representing the percent difference in tau phosphorylation between MK-801-treated mice and control mice were cross-normalized after calculating the relative baseline of phosphorylation of tau in different brain areas of the control mice. These results are presented in Figures 20 and 21.

Figures 20 and 21 show the extent of tau phosphorylation in different areas in the brain of the mice after analysis with PHF1 and CP13 and normalization to tubulin (100% represents the expression of phosphorylated tau protein in the cerebellum of the control mice.)

A systematic increase in tau phosphorylation was observed in all studied tissues after treating the mice with MK-801. For example, in the cortex the increase in phosphorylation in the 4 hour group was up to 20-fold.

The baseline induced degree of tau phosphorylation was also tissue specific. For example, the cortex showed the highest quantity of tau phosphorylation after the analysis with the PHF1 and CP13 antibodies. These results go along with the fact that the cortex is one of the most affected brain areas in Alzheimer´s disease and high numbers of neuropil threads (NTs) and neurofibrillary tangles (NFTs) were shown in the cortex in advanced stages of Alzheimer´s disease (Braak et al., 1999). Furthermore, the increase in tau phosphorylation started early in the cortex, i.e. two hours after the treatment when analyzed with the PHF1 antibody and one hour after the injection when analyzed with the CP13 antibody. These immediate baseline vulnerability data may correspond with Braak and colleagues which refer to NFTs and NTs occurring in the entorhinal and transentorhinal cortex (which are part of the medial temporal lobe) in the earliest stages of Alzheimer´s disease (stages I, II) (Braak and Braak 1991).

In contrast, the quantity of phosphorylated tau in the cerebellum after analysis with the PHF1 antibody started after two hours, but it was lower than in all other areas, and no significant increase in tau phosphorylation was observed after analysis with the CP13 antibody. This result is reminiscent of the fact that the cerebellum is less affected than other brain areas in Alzheimer´s disease and shows substantially less NTs/NFTs formation. Moreover, the control

group mice also showed a lower amount of baseline tau phosphorylation in the cerebellum in comparison to other brain areas (Figure 16). These results potentially explained by a low expression of tau protein kinases like MAPK and GSK-3ß in the cerebellum in comparison to other areas of the brain.

The phosphorylation in the hippocampus also started rapidly (one hour after the treatment with MK-801) (Figure 20) and thus faster than in all other areas, again resembling what is seen in Alzheimer´s disease, as NTs were found in the hippocampus in early stages of Alzheimer´s disease (Braak and Braak 1996). However, the peak of the amount of phosphorylated tau in the hippocampus was lower than in the cortex and the thalamus. One reason for this could be that the relatively small hippocampus is less dependent on axonal transport dynamic changes than the larger neocortex. Alternatively, the hippocampus may primarily use other mechanisms of NMDA receptor regulation than tau phosphorylation, such as amyloid formation: significant Aß amyloid production in the hippocampus has been documented in early stages of Alzheimer´s disease. Perhaps because of this mechanism, the phosphorylation of tau protein was not as high in the hippocampus as in the other areas of the brain. The study of amyloid production in the current mouse model might be interesting and might shed light on this question.

The phosphorylation of the tau protein in different areas of the brain also was epitope-specific and thus dependent on the different antibodies used (PHF1 and CP13). The phosphorylation of epitopes of PHF1 persisted in all examined areas until 24 hours after the injection of MK-801 (the half-life time of MK-801 was reported to be 2 h (Vezzani et al., 1989)). The reason might be that S396 and S404 epitope phosphorylation following MK-801 treatment is a long-term adaptation. According to Augustinack and colleagues, the PHF1 antibody stains iNFT, and its staining remains until the stage of formation of eNFT (Augustinack et al., 2002), which may also rationalize the persistence of the PHF1-phosphorylation detected here. Interestingly, the highest phosphorylation of the PHF1 epitope in the thalamus was detected after 24 hours, whereas in the cortex, peak phosphorylation was detected after two hours and then remained stable until 24 hours. These results could imply that not all S404 and S396 epitopes of the tau protein in the thalamus were phosphorylated after 24 hours, and that the highest amount of phosphorylation might only be detected after this time. In any case, the triggering cascade of tau phosphorylation appears to be relatively long-lived and stable after a short period of strong suppression of NMDAergic neurotransmission.

The detected increase in tau phosphorylation with the CP13 antibody, which detects tau phosphorylation at the S202 epitope, was highly dynamic. The peak of tau phosphorylation was detected in the thalamus and the cortex four hours after the treatment with MK-801 and

then declined after 24 hours. The reason for this observation might be that the phosphorylation at the S202 epitope is shorter, not as stable as the PHF1-epitope and gets hydrolyzed by phosphates more rapidly after the disappearance of MK-801. The highest amount of phosphorylation of the CP13 epitope among the studied areas was detected in the cortex four hours after the injection of MK-801.

Interestingly, the cerebellum did not show a systematic increase in tau phosphorylation at the CP13 epitope (Figure 21). However, an increase in tau phosphorylation was detected in the cerebellum with PHF1, which implies that blockade of NMDA receptor with MK-801 selectively enhanced the phosphorylation of the epitopes S396 and S404 in the cerebellum.

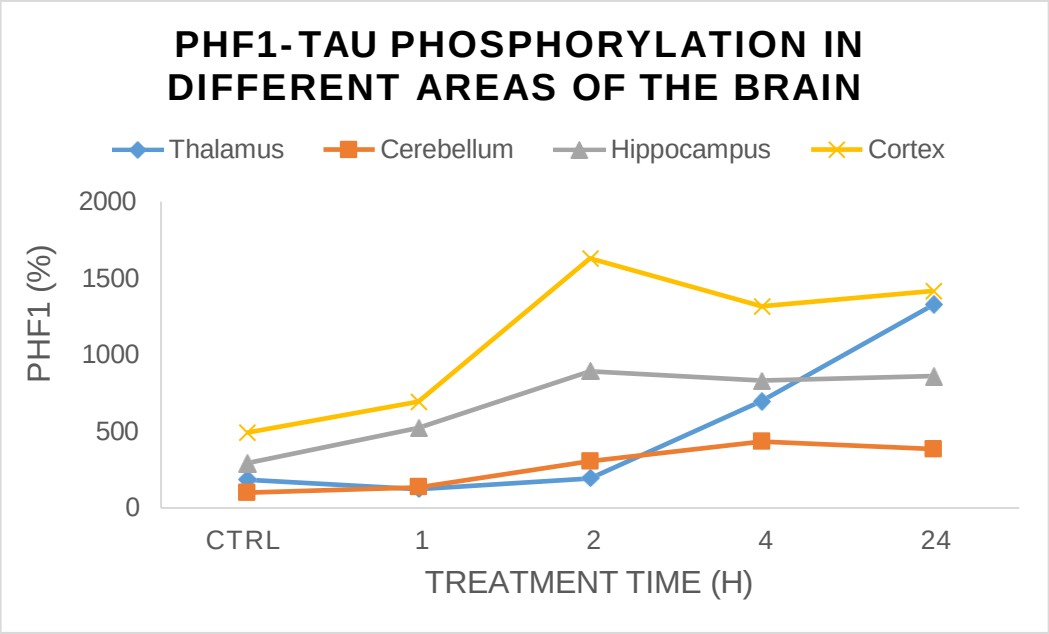

Figure 20: PHF1-tau phosphorylation in different areas of the brain.

Temporal course of tau phosphorylation in different areas of the brain of mice (the thalamus, the cerebellum, the hippocampus, and the cortex) after injection of MK-801, analysis with PHF1 and normalization to tubulin. The value 100 % represents tau phosphorylation in the cerebellum of the control mice. (The cortex data were generated by Sofie Meyer, BSc, during her master studies supervised by Prof. Bernd Moosmann).

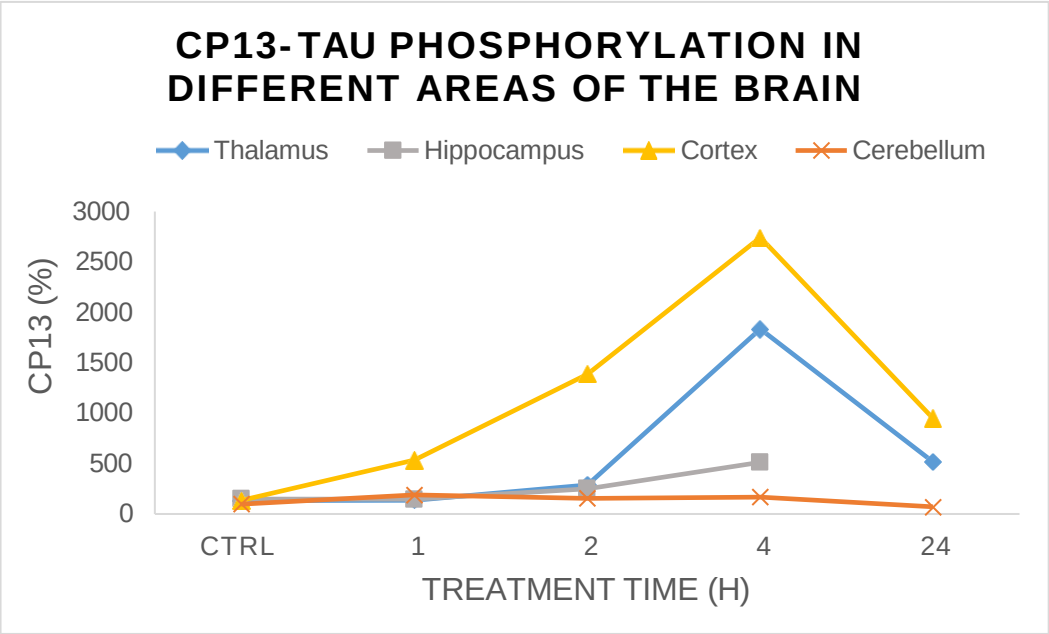

Figure 21: CP13-tau phosphorylation in different areas of the brain.

Temporal course of tau phosphorylation in different areas of the brain of mice (the thalamus, the hippocampus, and the cortex) after injection of MK-801, treatment with CP13 and normalization to tubulin. The amount of tau phosphorylation in the cerebellum of the control mice is represented by 100%. (Cortex data courtesy of Sofie Meyer, BSc).

4.5 NMDA receptors Hypofunction as Cause of Tau-Phosphorylation in Alzheimer Disease

It has already been shown that early hypoactivity of the excitatory system can lead to death of neuronal cells (Ikonomidou et al., 1999). Besides, some studies have proposed a role of NMDA receptors insufficiency in the progression of Alzheimer´s disease (Olney et al., 1997; Taffe et al., 2002). Furthermore, Wozniak and colleagues found a neurodegenerative pattern similar to that of Alzheimer´s disease in some areas of the rat cortex after application of a high dose of MK-801 (Wozniak et al. 1998; Horváth et al., 1997). However, a direct connection of NMDA receptors dysfunction to the pathological hallmarks of Alzheimer´s disease or their molecular predecessors has been missing.

This study provides evidence that the blockade of NMDA receptors with MK-801 leads to a pronounced increase in tau phosphorylation in different areas of the brain. Functionally, the described role of tau protein in the transport of NMDA receptors subunits and the activation of NMDA receptors by dendritic phospho-tau (Setou et al., 2000; Ittner et al., 2010) may constitute the purpose of the increased tau phosphorylation. This study proposes that the increase in tau

phosphorylation in many areas of the brain after inhibition of NMDA receptors could be a physiological compensatory mechanism to increase the excitatory neurotransmission after blocking NMDA receptors activation (Figure 22).

There are various risk factors associated with the emergence of Alzheimer's dementia. For several of these risk factors, there is a connection with impaired excitatory neurotransmission. For example, mutations of the Presenilin 1 gene (PS1) play a key role in hereditary Alzheimer´s disease. New studies suggest that PS1 gene mutations do not generally increase the production of Aß (Sun et al., 2017) but rather cause a deficit in neuronal development and a failure of the excitatory systems in the brain (Shen and Kelleher 2007; Heilig et al., 2010; Heilig et al., 2013). Presenilin also has been shown to be essential for the processes of learning, remembering and the survival of neuronal cells during the aging process (Saura et al., 2004; Wines-Samuelson et al., 2010; Xia et al., 2015). Mice with a human familial PS1 mutation have shown impairment of glutamatergic processes such as long-term plasticity (Xia et al., 2015). In addition, persistent NMDA receptors dysfunction has been described for mice with combined PS1/PS2 loss (Saura et al., 2004). These findings support the greatest suggestion of a role of NMDA receptors insufficiency in familial Alzheimer´s disease.

Another risk factor associated with Alzheimer´s disease is traumatic brain injury (TBI). Especially repeated TBI increases the risk of neurodegenerative diseases like Alzheimer´s disease (Jellinger 2004; Johnson et al., 2010; Ramos-Cejudo et al., 2018). A disseminated hyperphosphorylation and accumulation of tau in the brain after head trauma and TBI has been described (Edwards et al., 2017; Zanier et al., 2018). After TBI and stroke, NMDA receptors were initially hyperactivated, but then, within a brief time period, a secondary loss of functional NMDA receptors was observed which persisted for weeks (Ogawa et al., 1991; Grossman et al., 2003; Biegon et al., 2004; Shohami and Biegon 2014). It is the neuronal axons that are primarily affected after traumatic injury, and tau protein is known for its central role in the regulation of axonal transport and microtubule stability. Therefore, the tau protein and its phosphorylation might play a role in the post-TBI reorganization and repair of damaged, disconnected axons.

Furthermore, the pathological features that occur in Alzheimer's dementia are often seen in other diseases caused by varying triggers as well. Upon closer inspection, these features appear to be rather general responses rather than exclusively Alzheimer's-specific signatures, as the occurrence of NFTs is also observed in frontotemporal dementia (Gordon et al., 2016), in survivors of untreated encephalitis (Arendt 2003) or in trisomy 21 patients (Down Syndrome patients) (Wiseman et al., 2015). The general occurrence of tau phosphorylation and NFTs in various neuronal-associated diseases supports the suggestion that the increase in tau

phosphorylation is a molecular compensatory response to a more universal trigger, namely excitatory insufficiency (Figure 22).

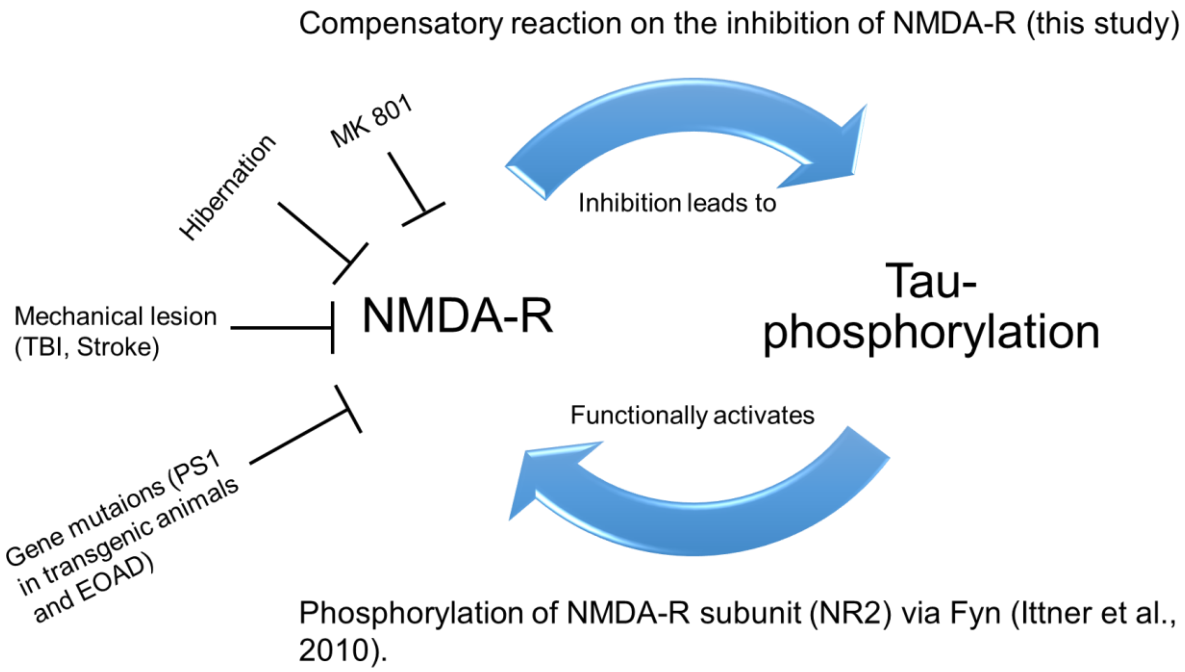

Figure 22: NMDA receptors insufficiency and tau phosphorylation.

Tau protein interacts with the kinase Fyn, which in turn phosphorylates the NMDA receptor subunit 2 (NR2) and activates NMDA receptors. In contrast, the inhibition of NMDA receptors in consequence of different physiological and pathological events (hibernation, TBI, stroke, NMDA receptor antagonism and PS1 mutations) and their function in memory and learning can initiate tau phosphorylation as a compensatory reaction to increase the excitatory neurotransmission.

As a conclusion, this study strongly suggests a role for NMDA receptor insufficiency in the development of tau pathology in Alzheimer´s disease. To complement the presented research, the effect of inhibiting AMPA and other neuroexcitatory receptors on the phosphorylation of tau should be analyzed. Moreover, it should be studied if NMDA receptor hypofunction also plays a role in Aß pathology. Furthermore, immunohistochemistry could be used to detect the phosphorylation of tau and the potential formation of NFTs and NTs in different areas of the brain at the single-cell resolution level. As a long-term goal, it should be investigated which reasons lead to the potential inhibition of NMDA receptor in the early stages of Alzheimer´s disease, before the development of clinical symptoms, to identify molecular targets for clinical studies aimed at the prevention and treatment of this devastating disease.

5. Zusammenfassung

Die Alzheimer-Krankheit ist eine der wichtigsten neurodegenerativen Erkrankungen und die häufigste Form der Demenz beim Menschen. Die Prävalenz der Alzheimer-Krankheit steigt mit dem Alter. Die Pathophysiologie der Alzheimer-Krankheit ist noch nicht vollständig verstanden. Intrazelluläre neurofibrilläre Bündel (NFTs) aus hyperphosphorlyiertem Tau-Protein sind ein wichtiges pathologisches Merkmal der Alzheimer-Krankheit. Der Beginn der Tau-Phosphorylierung und deren entscheidende molekulare Auslöser sind bislang unklar. NMDA Rezeptoren sind exzitatorische Rezeptoren im Gehirn, die eine wichtige Rolle für Gedächtnis und Lernen spielen. Die vorliegende Studie zeigt die Wirkung einer Hemmung von NMDA Rezeptoren auf die Induktion der Tau-Phosphorylierung in vivo auf und analysiert erstmals die spatio-temporale Dynamik dieser Induktion.

Für die vorliegende Studie wurden 25 Mäuse in fünf verschiedene Behandlungsgruppen zu je fünf Mäusen aufgeteilt. Die Saline Kontrollgruppe erhielt keine Wirkstoff-Behandlung, während die anderen Gruppen für eine, zwei, vier oder 24 Stunden mit dem nicht-kompetitiven NMDA-Antagonisten MK-801 behandelt wurden. Aus den Gehirnen der Mäuse wurden Lysate angefertigt und anschließend mittels Western Blot analysiert. Zwei Antikörper (PHF1 und CP13) wurden verwendet, um die Phosphorylierung des Tau-Proteins in drei verschiedenen Gebieten des Gehirns (Thalamus, Hippocampus und Cerebellum) zu detektieren. Diese Antikörper erkennen die Phosphorylierung des Tau-Proteins an erkrankungsspezifischen Epitopen; PHF1 erkennt die Tau-Phosphorylierung an S396 und S404, und CP13 erkennt die Phosphorylierung an S202. Die Ergebnisse wurden quantifiziert, auf Tubulin oder das gesamte Tau-Protein normiert und statistisch ausgewertet.

Die Analyse der Ergebnisse zeigte eine Zunahme der Tau-Phosphorylierung in allen drei Gehirnarealen nach der Behandlung mit MK-801. Die Phosphorylierung stieg Antikörper-spezifisch zu unterschiedlichen Zeitpunkten in den verschiedenen Bereichen des Gehirns an. Die früheste Reaktion wurde im Hippocampus mit dem PHF1 Antikörper beobachtet; hier begann die Reaktion bereits eine Stunde nach der Injektion von MK-801. Das Ausmaß der Zunahme der Tau-Phosphorylierung variierte ebenfalls von Gebiet zu Gebiet. Der höchste Anstieg der Tau-Phosphorylierung im Vergleich zur Kontrollgruppe wurde im Thalamus mit dem CP13-Antikörper in der Vier-Stunden-Gruppe festgestellt. Ein hochsignifikanter Anstieg der Tau-Phosphorylierung ($p < 0,001$) wurde im Thalamus mit dem PHF1 Antikörper in der 24-Stunden-Gruppe, im Hippocampus mit dem CP13-Antikörper in der Vier-Stunden-Gruppe und im Cerebellum mit dem PHF1 Antikörper in der Vier-Stunden-Gruppe beobachtet.

Der manifeste Anstieg der Tau-Phosphorylierung in verschiedenen Gebieten des Gehirns könnte einen kompensatorischen Mechanismus darstellen, der der auslösenden Hemmung der exzitatorischen Neurotransmission entgegengerichtet ist. Dies ist plausibel, da mehrere Publikationen einen pro-exzitatorischen Effekt des phosphorylierten Tau-Proteins gezeigt haben. Die hier vorgelegte Arbeit legt nahe, dass chronische Hypoaktivität der NMDA Rezeptoren ein molekularer Auslöser der Tau-Phosphorylierung in frühen Phasen der Alzheimer-Krankheit sein könnte. Um diesen Befund zu erweitern, wäre es wichtig, auch die Effekte einer Hemmung der NMDA Rezeptoren auf die Amyloid-Prozessierung und die mögliche Bildung von extrazellulären Plaques des Aß-Peptids zu untersuchen. Mittelfristig wäre es weiterhin wichtig, diejenigen Faktoren zu identifizieren, die am ehesten eine chronische Hemmung der NMDA Rezeptoren in vivo vermitteln. Die präventive oder therapeutische Elimination dieser Faktoren könnte möglicherweise die Entstehung der Alzheimer-Krankheit verzögern oder verhindern.

5. Summary

Alzheimer's disease is one of the most important neurodegenerative disorders and the most common form of dementia in humans. The prevalence of Alzheimer´s disease increases with age. The pathophysiology of Alzheimer´s disease is not completely understood yet. Intracellular neurofibrillary tangles of phosphorylated tau protein are an important pathological characteristic of Alzheimer´s disease. The beginning of tau phosphorylation and its molecular triggers remain unclear. NMDA receptors are excitatory receptors in the brain that play an important role in memory and learning. The current study demonstrated the effects of an inhibition of NMDA receptors on the induction of tau phosphorylation in vivo and, for the first time, provided an analysis of the spatio-temporal dynamic of this induction.

To study the effect of NMDA receptors on the induction of tau phosphorylation, 25 mice were allocated to five different treatment groups of five mice each. The control group received vehicle (saline), while the other groups were treated with the non-competitive NMDA antagonist MK-801 for one, two, four, and 24 hours. Lysates were prepared from the brains of the treated mice and analyzed by Western blotting. Two antibodies (PHF1 and CP13) were used to detect the phosphorylation of the tau protein in three different areas of the brain (the thalamus, the hippocampus, and the cerebellum). These antibodies detect the phosphorylation of the tau protein at disease-relevant, specific epitopes; PHF1 detects tau phosphorylation at S396 and S404, and CP13 detects phosphorylation at S202. The results were quantified, normalized to tubulin or total tau protein and evaluated statistically.

Analysis of the results evidenced an increase in tau phosphorylation in all three areas of the brain after treatment with MK-801. The phosphorylation started at different times in the different areas and varied pursuant to the employed antibodies. The fastest response was observed in the hippocampus with the PHF1 antibody; here, increase phosphorylation started already one hour after the injection of MK-801. The degree of the increase in tau phosphorylation also varied from area to area; the peak in tau phosphorylation compared to the control group was detected in the thalamus with the CP13 antibody in the 4 hour treatment group. A highly significant increase in tau phosphorylation ($p < 0.001$) was observed in the thalamus with the PHF1 antibody in the 24 hour group, in the hippocampus with the CP13 antibody in the 4 hour group, and in the cerebellum with the PHF1 antibody in the 4 4hour group.

The observed increase in tau phosphorylation in different areas of the brain of mice could represent a compensatory mechanism to counteract the triggering inhibition of NMDAergic excitatory neurotransmission, because a facilitation of excitatory neurotransmission by phosphorylated tau protein has been demonstrated before. The current study suggests that chronic NMDA receptor hypoactivity could be a molecular trigger of tau phosphorylation in prodromal Alzheimer´s disease. To complement this research, the effects of the inhibition of NMDA receptors on amyloid processing and the formation of extracellular plaques of the Aβ-peptide should be studied. In the medium term, it will be important to identify any factors that might chronically inhibit NMDA receptor activity in vivo. Control of these factors may offer a new strategy to delay or prevent the development of Alzheimer´s disease.

6. References

- Ahmed H, Haider A, Ametamey SM (2020). N-Methyl-D-Aspartate (NMDA) receptor modulators: a patent review (2015-present). Expert Opin Ther Pat. 30 (10):743-767.
- Allen HL, Iversen LL (1990). Phencyclidine, dizocilpine, and cerebrocortical neurons. Science. 247:221.
- Alzheimer A (1907). Über eine eigenartige Erkrankung der Hirnrinde. Allg Z Psychiatr. 64: 146-148.
- Alzheimer's Association (2011). Alzheimer's disease facts and figures. Alzheimers Dement 7: 208-244.
- Alzheimer's Association (2018). Alzheimer's disease facts and figures. Alzheimers Dement. 14(3):367–429.
- Alzheimer's Association (2019). Alzheimer's disease facts and figures. Alzheimers Dement 15: 321–387.
- Anand KS, Dhikav V (2012). Hippocampus in health and disease: An overview. Ann Indian Acad Neurol. 15(4):239-246.
- Andiné P, Widermark N, Axelsson R, Nyberg G, Olofsson U, Mårtensson E, Sandberg M (1999). Characterization of MK-801-induced behavior as a putative rat model of psychosis. J Pharmacol Exp Ther. 290(3):1393-1408.
- Arendt T (2003). Synaptic plasticity and cell cycle activation in neurons are alternative effector pathways: the 'Dr. Jekyll and Mr. Hyde concept' of Alzheimer's disease or the yin and yang of neuroplasticity. Prog Neurobiol. 71(2-3):83-248.
- Arendt T, Stieler J, Strijkstra AM, Hut RA, Rüdiger J, Van der Zee EA, Harkany T, Holzer M, Härtig W (2003). Reversible paired helical filament-like phosphorylation of tau is an adaptive process associated with neuronal plasticity in hibernating animals. J Neurosci. 23(18):6972-6981.
- Augustinack JC, Schneider A, Mandelkow EM, Hyman BT (2002). Specific tau phosphorylation sites correlate with severity of neuronal cytopathology in Alzheimer's disease. Acta Neuropathol. 103(1):26-35.
- Bakker CB, Amini FB (1961). Observations on the psychotomimetic effects of Sernyl. Compr Psychiatry. 2:269-280.
- Beher D, Elle C, Underwood J, Davis JB, Ward R, Karran E, Masters CL, Beyreuther K, Multhaup G (1999). Proteolytic fragments of Alzheimer's disease-associated presenilin 1 are present in synaptic organelles and growth cone membranes of rat brain. J Neurochem. 72(4):1564-1573.
- Bekris LM, Yu CE, Bird TD Tsuang DW (2010). Genetics of Alzheimer disease. J Geriatr Psychiatry Neurol. 23(4): 213-227.
- Benarroch EE (2011). NMDA receptors: recent insights and clinical correlations. Neurology. 76(20):1750-1757.

- Biegon A, Fry PA, Paden CM, Alexandrovich A, Tsenter J, Shohami E (2004). Dynamic changes in N-methyl-D-aspartate receptors after closed head injury in mice: Implications for treatment of neurological and cognitive deficits. Proc Natl Acad Sci U S A. 101(14):5117-5122
- Bliss TV, Collingridge GL (1993). A synaptic model of memory: long-term potentiation in the hippocampus. Nature. 361(6407):31-39.
- Braak E, Griffing K, Arai K, Bohl J, Bratzke H, Braak H (1999). Neuropathology of Alzheimer's disease: what is new since A. Alzheimer? Eur Arch Psychiatry Clin Neurosci. 249 Suppl 3:14-22.
- Braak H, Braak E (1991). Neuropathological stageing of Alzheimer-related changes. Acta Neuropathol. 82(4):239-259
- Braak H, Braak E (1994). Pathology of Alzheimer's disease. In: Calne DB (ed) neurodegenerative diseases. Saunders, Philadelphia, pp 585–613.
- Braak H, Braak E (1996). Development of Alzheimer-related neurofibrillary changes in the neocortex inversely recapitulates cortical myelogenesis. Acta Neuropathol 92: 197–201.
- Braak H, Braak E (1997). Frequency of stages of Alzheimer-related lesions in different age categories. Neurobiol Aging 18: 351–357.
- Braak H, Thal DR, Ghebremedhin E, Del Tredici K (2011). Stages of the pathologic process in Alzheimer disease: age categories from 1 to 100 years. J Neuropathol Exp Neurol. 70(11):960-969.
- Capell A, Meyn L, Fluhrer R, Teplow DB, Walter J, Haass C (2002). Apical sorting of beta-secretase limits amyloid beta-peptide production. J Biol Chem. 277(7):5637-5643.
- Chen XH, Siman R, Iwata A, Meaney DF, Trojanowski JQ, Smith DH (2004). Long-term accumulation of amyloid-beta, beta-secretase, presenilin-1, and caspase-3 in damaged axons following brain trauma. Am J Pathol. 165(2):357-371.
- Crystal JD (2020). Memory: Amyloid Beta Is Good Before It Is Bad. Curr Biol. 18;30(10):449-450.
- Davies BM, Beech HL (1960). The effect of 1-arylcyclohexylamine (Sernyl) on 12 normal volunteers. J Ment Sci. 106:912-924.
- Dhikav V, Anand KS (2012). Are vascular factors linked to the development of hippocampal atrophy in Alzheimer's disease? J Alzheimers Dis. 32(3):711-718.
- Dixit R, Ross JL, Goldman YE, Holzbaur EL (2008). Differential regulation of dynein and kinesin motor proteins by tau. Science. 319(5866):1086-1089.
- Edwards G 3rd, Moreno-Gonzalez I, Soto C (2017). Amyloid-beta and tau pathology following repetitive mild traumatic brain injury. Biochem Biophys Res Commun. 19;483(4):1137-1142.
- Farlow MR, Cummings JL (2007). Effective pharmacologic management of Alzheimer's disease. Am J Med 120(5):388–397.
- Fischer O (1907). Miliare Nekrosen mit drusigen Wucherungen der Neurofibrillen, eine regelmässige Veränderung der Hirnrinde bei seniler Demenz. Monatsschr Psychiat Neurol. 22, 361–372.

- Frisoni GB, Fox NC, Jack CR Jr, Scheltens P, Thompson PM (2010). The clinical use of structural MRI in Alzheimer disease. Nat Rev Neurol. 6:67-77.
- Furukawa K, Guo Q, Schellenberg GD, Mattson MP (1998). Presenilin-1 mutation alters NGF-induced neurite outgrowth, calcium homeostasis, and transcription factor (AP-1) activation in PC12 cells. J Neurosci Res. 52(5):618-624.
- Garcia-Osta A, Alberini CM. (2009) Amyloid beta mediates memory formation. Learn Mem. 16(4):267-272.
- Gardoni, F.; Mauceri, D.; Malinverno, M.; Polli, F.; Costa, C.; Tozzi, A.; Siliquini, S.; Picconi, B.; Cattabeni, F.; Calabresi, P.; Di Luca, M (2009). Decreased NR2B subunit synaptic levels cause impaired long-term potentiation but not long-term depression. J. Neurosci. 29 (3), 669-677.
- Geschwind, DH (2003). Tau phosphorylation, tangles, and neurodegeneration: the chicken or the egg? Neuron 40, 457–460.
- Gilbert PE, Brushfield AM (2009). The role of the CA3 hippocampal subregion in spatial memory: A process oriented behavioral assessment. Prog Neuropsychopharmacol Biol Psychiatry. 33:774-781.
- Gonzalez-Lima F, Berndt JD, Valla JE, Games D, Reiman EM (2001). Reduced corpus callosum, fornix and hippocampus in PDAPP transgenic mouse model of Alzheimer's disease. Neuroreport. 12(11):2375-2379.
- Gordon E, Rohrer JD, Fox NC (2010). Advances in neuroimaging in frontotemporal dementia. J Neurochem. 138 Suppl 1:193-210.
- Greenberg SG, Davies P, Schein JD, Binder LI (1992). Hydrofluoric acid-treated tau PHF proteins display the same biochemical properties as normal tau. J Biol Chem. 267:564–569.
- Grossman R, Shohami E, Alexandrovich A, Yatsiv I, Kloog Y, Biegon A (2003). Increase in peripheral benzodiazepine receptors and loss of glutamate NMDA receptors in a mouse model of closed head injury: a quantitative autoradiographic study. Neuroimage. 20(4):1971-1981
- Grundke-Iqbal I, Iqbal K, Tung Y, Quinlan M, Wisniewski H, Binder L (1986). Abnormal phosphorylation of the microtubule-associated protein tau (tau) in Alzheimer cytoskeletal pathology. Proc Natl Acad Sci U S A. 83: 4913-4917.
- Haass C (2004). Take five-BACE and the gamma-secretase quartet conduct Alzheimer's amyloid beta-peptide generation. EMBO J. 23(3):483-488.
- Haass C, Schlossmacher MG, Hung AY, Vigo-Pelfrey C, Mellon A, Ostaszewski BL, Lieberburg I, Koo EH, Schenk D, Teplow DB, et al (1992). Amyloid beta-peptide is produced by cultured cells during normal metabolism. Nature 359(5393), 322–325.
- Haass, C. and Selkoe, DJ (2007). Soluble protein oligomers in neurodegeneration: Lessons from the Alzheimer's amyloid b-peptide. Nat. Rev. Mol. Cell Biol. 8: 101–112.
- Hajieva P, Moosmann B (2015). Brain protein oxidation: what does it reflect? Neural Regen Res. 10(11):1729-1730.

- Hefti MM, Kim S, Bell AJ, Betters RK, Fiock KL, Iida MA, Smalley ME, Farrell K, Fowkes ME, Crary JF (2009). Tau Phosphorylation and Aggregation in the Developing Human Brain. J Neuropathol Exp Neurol. 78(10):930-938.
- Heilig EA, Gutti U, Tai T, Shen J, Kelleher RJ 3rd (2013). Trans-dominant negative effects of pathogenic PSEN1 mutations on γ-secretase activity and Aβ production. J Neurosci. 33(28):11606-11617.
- Heilig EA, Xia W, Shen J, Kelleher RJ 3rd (2010). A presenilin-1 mutation identified in familial Alzheimer disease with cotton wool plaques causes a nearly complete loss of gamma-secretase activity. J Biol Chem. 285(29):22350-22359.
- Hernandez P, Lee G, Sjoberg M, Maccioni R (2009). Tau phosphorylation by cdk5 and Fyn in response to amyloid peptide Abeta (25-35): involvement of lipid rafts. J Alzheimers Dis. 16: 149-156.
- Herrero MT, Barcia C, Navarro JM (2002). Functional anatomy of thalamus and basal ganglia. Childs Nerv Syst. 18(8):386-404.
- Horváth ZC, Czopf J, Buzsáki G (1997). MK-801-induced neuronal damage in rats. Brain Res. 753(2):181-195.
- Hsiao K, Chapman P, Nilsen S, Eckman C, Harigaya Y, Younkin S, Yang F, Cole G (1996). Correlative memory deficits, Abeta elevation, and amyloid plaques in transgenic mice. Science. 274(5284):99-102.
- Huang YJ, Lin CH, Lane HY, Tsai GE (2012). NMDA Neurotransmission Dysfunction in Behavioral and Psychological Symptoms of Alzheimer's Disease. Curr Neuropharmacol. 10(3):272-785.
- Hucker HB, Hutt JE, White SD, Arison BH, Zacchei AG (1983). Disposition and metabolism of (+)-5-methyl-10,11-dihydro-5H-dibenzo[a,d] cyclohepten-5,10-imine in rats, dogs, and monkeys. Drug Metab Dispos. 11(1):54-58.
- Hyman BT (1998). New neuropathological criteria for Alzheimer’s disease. Arch Neurol 55: 1174–1176.
- Hyman BT, Gomez-Isla T (1994). Alzheimer’s disease is a laminar, regional, and neural system specific disease, not a global brain disease. Neurobiol Aging 15: 353–354.
- Iijima K, Gatt A, Iijima-Ando K (2010). Tau Ser262 phosphorylation is critical for Abeta42-induced tau toxicity in a transgenic Drosophila model of Alzheimer's disease. Hum Mol Genet. 19: 2947-2957.
- Ikonomidou C, Bosch F, Miksa M, Bittigau P, Vöckler J, Dikranian K, Tenkova TI, Stefovska V, Turski L, Olney JW (1999). Blockade of NMDA receptors and apoptotic neurodegeneration in the developing brain. Science. 283(5398):70-74.
- Illenberger S, Zheng-Fischhöfer Q, Preuss U, Stamer K, Baumann K, Trinczek B, Biernat J, Godemann R, Mandelkow EM, Mandelkow E (1998). The endogenous and cell cycle-dependent phosphorylation of tau protein in living cells: implications for Alzheimer's disease. Mol Biol Cell. 9(6):1495-1512.

- Ittner LM, Ke YD, Delerue F, Bi M, Gladbach A, van Eersel J, Wölfing H, Chieng BC, Christie MJ, Napier IA, Eckert A, Staufenbiel M, Hardeman E, Götz J (2010). Dendritic function of tau mediates amyloid-beta toxicity in Alzheimer's disease mouse models. Cell. 142(3):387-397.
- Iwai A, Masliah E, Yoshimoto M, Ge N, Flanagan L, de Silva HA, Kittel A, Saitoh T (1995). The precursor protein of non-A beta component of Alzheimer's disease amyloid is a presynaptic protein of the central nervous system. Neuron. 14(2):467-475.
- Jacobs HIL, Hopkins DA, Mayrhofer HC, Bruner E, van Leeuwen FW, Raaijmakers W, Schmahmann JD (2018). The cerebellum in Alzheimer's disease: evaluating its role in cognitive decline. Brain. 141(1):37-47.
- Javitt DC, Zukin SR (1991). Recent advances in the phencyclidine model of schizophrenia. Am J Psychiatry. 148:1301-1308.
- Jellinger KA (2004). Head injury and dementia. Curr Opin Neurol. 17(6):719-723.
- Johnson VE, Stewart W, Smith DH (2010). Traumatic brain injury and amyloid-β pathology: a link to Alzheimer's disease? Nat Rev Neurosci. 11(5):361-370.
- Jost BC, Grossberg GT(1995). The natural history of Alzheimer’s disease: a brain bank study. J Am Geriatr Soc 43(11):1248–1255.
- Jost BC, Grossberg GT(1996). The evolution of psychiatric symptoms in Alzheimer’s disease: a natural history study. J Am Geriatr Soc 44(9):1078–1081.
- Kalia LV, Kalia SK, Salter MW (2008). NMDA receptors in clinical neurology: excitatory times ahead. Lancet Neurol. 7 (8), 742-755.
- Kamal A, Stokin GB, Yang Z, Xia CH, Goldstein LS (2000). Axonal transport of amyloid precursor protein is mediated by direct binding to the kinesin light chain subunit of kinesin-I. Neuron. 28(2):449-459.
- Karch CM, Goate AM (2015). Alzheimer’s disease risk genes and mechanisms of disease pathogenesis. Biol Psychiatry 77: 43–51.
- Kimura T, Ono T, Takamatsu J, Yamamoto H, Ikegami K, Kondo A, Hasegawa M, Ihara Y, Miyamoto E, Miyakawa T (1996). Sequential changes of tau-site-specific phosphorylation during development of paired helical filaments. Dementia. 7:177–181.
- Kojro E, Fahrenholz F (2005). The non-amyloidogenic pathway: structure and function of alpha-secretases. Subcell Biochem. 38:105-127.
- Koo EH, Sisodia SS, Archer DR, Martin LJ, Weidemann A, Beyreuther K, Fischer P, Masters CL, Price DL (1990). Precursor of amyloid protein in Alzheimer disease undergoes fast anterograde axonal transport. Proc Natl Acad Sci U S A. 87(4):1561-1565.
- Kovacic P, Somanathan R (2010). Clinical physiology and mechanism of dizocilpine (MK-801): electron transfer, radicals, redox metabolites and bioactivity. Oxid Med Cell Longev. 3(1):13-22.
- Lambert JC, Ibrahim-Verbaas CA, Harold D, Naj AC, Sims R, Bellenguez C, DeStafano AL, Bis JC, Beecham GW, Grenier-Boley B, Russo G, Thorton-Wells TA, Jones N, Smith AV, Chouraki V, Thomas C, Ikram MA, Zelenika D, Vardarajan BN, Kamatani Y, Lin CF, Gerrish A, Schmidt H, Kunkle B, Dunstan ML, Ruiz A, Bihoreau MT, Choi SH, Reitz C, Pasquier F, Cruchaga C, Craig

D, Amin N, Berr C, Lopez OL, De Jager PL, Deramecourt V, Johnston JA, Evans D, Lovestone S, Letenneur L, Morón FJ, Rubinsztein DC, Eiriksdottir G, Sleegers K, Goate AM, Fiévet N, Huentelman MW, Gill M, Brown K, Kamboh MI, Keller L, Barberger-Gateau P, McGuiness B, Larson EB, Green R, Myers AJ, Dufouil C, Todd S, Wallon D, Love S, Rogaeva E, Gallacher J, St George-Hyslop P, Clarimon J, Lleo A, Bayer A, Tsuang DW, Yu L, Tsolaki M, Bossù P, Spalletta G, Proitsi P, Collinge J, Sorbi S, Sanchez-Garcia F, Fox NC, Hardy J, Deniz Naranjo MC, Bosco P, Clarke R, Brayne C, Galimberti D, Mancuso M, Matthews F; European Alzheimer's Disease Initiative (EADI); Genetic and Environmental Risk in Alzheimer's Disease; Alzheimer's Disease Genetic Consortium; Cohorts for Heart and Aging Research in Genomic Epidemiology; Moebus S, Mecocci P, Del Zompo M, Maier W, Hampel H, Pilotto A, Bullido M, Panza F, Caffarra P, Nacmias B, Gilbert JR, Mayhaus M, Lannefelt L, Hakonarson H, Pichler S, Carrasquillo MM, Ingelsson M, Beekly D, Alvarez V, Zou F, Valladares O, Younkin SG, Coto E, Hamilton-Nelson KL, Gu W, Razquin C, Pastor P, Mateo I, Owen MJ, Faber KM, Jonsson PV, Combarros O, O'Donovan MC, Cantwell LB, Soininen H, Blacker D, Mead S, Mosley TH Jr, Bennett DA, Harris TB, Fratiglioni L, Holmes C, de Bruijn RF, Passmore P, Montine TJ, Bettens K, Rotter JI, Brice A, Morgan K, Foroud TM, Kukull WA, Hannequin D, Powell JF, Nalls MA, Ritchie K, Lunetta KL, Kauwe JS, Boerwinkle E, Riemenschneider M, Boada M, Hiltuenen M, Martin ER, Schmidt R, Rujescu D, Wang LS, Dartigues JF, Mayeux R, Tzourio C, Hofman A, Nöthen MM, Graff C, Psaty BM, Jones L, Haines JL, Holmans PA, Lathrop M, Pericak-Vance MA, Launer LJ, Farrer LA, van Duijn CM, Van Broeckhoven C, Moskvina V, Seshadri S, Williams J, Schellenberg GD, Amouyel P (2013). Meta-analysis of 74,046 individuals identifies 11 new susceptibility loci for Alzheimer's disease. Nat Genet. 45(12):1452-8.

- Lee EB, Zhang B, Liu K, Greenbaum EA, Doms RW, Trojanowski JQ, Lee VM (2005). BACE overexpression alters the subcellular processing of APP and inhibits Abeta deposition in vivo. J Cell Biol. 168(2):291-302.
- Lei G, Xia Y, Johnson KM (2008). The role of Akt-GSK-3beta signaling and synaptic strength in phencyclidine-induced neurodegeneration. Neuropsychopharmacology. 33(6):1343-1353.
- Leyssen M, Ayaz D, Hébert SS, Reeve S, De Strooper B, Hassan BA (2005). Amyloid precursor protein promotes post-developmental neurite arborization in the Drosophila brain. EMBO J. 24(16):2944-2955.
- Lisman J, Buzsáki G, Eichenbaum H, Nadel L, Ranganath C, Redish AD (2017). Viewpoints: how the hippocampus contributes to memory, navigation and cognition. Nat Neurosci. 20(11):1434-1447.
- Lopez OL, Chang Y, Ives DG, Snitz BE, Fitzpatrick AL, Carlson MC, Rapp SR, Williamson JD, Tracy RP, DeKosky ST, Kuller LH (2019). Blood amyloid levels and risk of dementia in the Ginkgo Evaluation of Memory Study (GEMS): A longitudinal analysis. Alzheimers Dement. 15(8):1029-1038.
- Madden K (2002). NMDA receptor antagonists and glycine site NMDA antagonists. Curr Med Res Opin. 18 Suppl 2:27-31.

- Maeda S, Djukic B, Taneja P, Yu GQ, Lo I, Davis A, Craft R, Guo W, Wang X, Kim D, Ponnusamy R, Gill TM, Masliah E, Mucke L (2016). Expression of A152T human tau causes age-dependent neuronal dysfunction and loss in transgenic mice. EMBO Rep. 17(4):530-551.
- Magara F, Müller U, Li ZW, Lipp HP, Weissmann C, Stagljar M, Wolfer DP (1999). Genetic background changes the pattern of forebrain commissure defects in transgenic mice underexpressing the beta-amyloid-precursor protein. Proc Natl Acad Sci U S A. 96(8):4656-4661.
- Magnusson KR, Sammonds GE (1998). Age-related changes in the expression of NMDA receptor subunits. FASEB J. 12:4365.
- Masliah E, Mallory M, Ge N, Saitoh T (1992). Amyloid precursor protein is localized in growing neurites of neonatal rat brain. Brain Res. 593(2):323-328.
- Mayer ML (2006). Glutamate receptors at atomic resolution. Nature. 440(7083):456-462.
- McDonald AJ, Mott DD (2017). Functional neuroanatomy of amygdalohippocampal interconnections and their role in learning and memory. J Neurosci Res. 95(3):797-820.
- McGeer PL, McGeer EG, Akiyama H, Itagaki S, Harrop R, Peppard R (1990). Neuronal degeneration and memory loss in Alzheimer's disease and aging. Exp Brain Res (Suppl) 21: 411– 426.
- Mielke M, Vemuri P, Rocca W (2014). Clinical epidemiology of Alzheimer´s disease: assessing sex and gender differences. Clinical Epidemiology. 6:37-48.
- Minoshima S, Giordani B, Berent S, Frey KA, Foster NL, Kuhl DE (1997). Metabolic reduction in the posterior cingulate cortex in very early Alzheimer's disease. Ann Neurol. 42(1):85-94.
- Mishizen-Eberz AJ, Rissman RA, Carter TL, Ikonomovic MD, Wolfe BB, Armstrong DM (2004). Biochemical and molecular studies of NMDA receptor subunits NR1/2A/2B in hippocampal subregions throughout progression of Alzheimer's disease pathology. Neurobiol. Dis. 15 (1), 80-92.
- Monyer H, Burnashev N, Laurie DJ, Sakmann B, Seeburg PH (1994). Developmental and regional expression in the rat brain and functional properties of four NMDA receptors. Neuron. 12:529-540.
- Morley JE, Farr SA (2014). The role of amyloid-beta in the regulation of memory. Biochem Pharmacol. 88(4):479-485.
- Newcomer JW, Farber NB, Olney JW (2000). NMDA receptor function, memory, and brain aging. Dialogues Clin Neurosci. 2(3):219-232.
- Nicolas M, Hassan BA (2014). Amyloid precursor protein and neural development. Development. 141(13):2543-2548.
- Niewiadomska G, Baksalerska-Pazera M, Riedel G (2009). The septo- hippocampal system, learning and recovery of function. Prog Neuropsychopharmacol Biol Psychiatry. 33(5):791-805.
- Ogawa N, Haba K, Mizukawa K, Asanuma M, Hirata H, Mori A (1991). Loss of N-methyl- D-aspartate (NMDA) receptor binding in rat hippocampal areas at the chronic stage after transient

forebrain ischemia: Histological and NMDA receptor binding studies. Neurochem Res. 16(5): 519-524.

- Ohm TG (1997). Does Alzheimer's disease start early in life? Molecular Psychiatry 2: 21–25.
- Ohm TG, Müller H, Braak H, Bohl J (1995). Close-meshed prevalence rates of different stages as a tool to uncover the rate of Alzheimer's disease-related neurofibrillary changes. Neuroscience 64: 209–217.
- Olney JW, Labruyere J, Price MT (1989). Pathological changes induced in cerebrocortical neurons by phencyclidine and related drugs. Science. 244(4910):1360-1362.
- Olney JW, Wozniak DF, Farber NB (1997). Excitotoxic neurodegeneration in Alzheimer disease. New hypothesis and new therapeutic strategies. Arch Neurol. 54(10):1234-1240.
- Petersen RC, Lopez O, Armstrong MJ, Getchius TSD, Ganguli M, Gloss D, Gronseth GS, Marson D, Pringsheim T, Day GS, Sager M, Stevens J, Rae-Grant A (2018). Practice guideline update summary: Mild cognitive impairment [RETIRED]: Report of the Guideline Development, Dissemination, and Implementation Subcommittee of the American Academy of Neurology. Neurology. 2018 90(3):126-135.
- Petry FR, Pelletier J, Bretteville A, Morin F, Calon F, Hébert SS, Whittington RA, Planel E (2014). Specificity of anti-tau antibodies when analyzing mice models of Alzheimer's disease: problems and solutions. PLoS One. 9(5): e94251.
- Procter AW, Wong EH, Stratmann GC, Lowe SL, Bowen D (1989). M. Reduced glycine stimulation of [3H]MK-801 binding in Alzheimer's disease. J. Neurochem. 53 (3), 698-704.
- Ramos-Cejudo J, Wisniewski T, Marmar C, Zetterberg H, Blennow K, de Leon MJ, Fossati S (2018). Traumatic Brain Injury and Alzheimer's Disease: The Cerebrovascular Link. EBioMedicine. 28:21-30.
- Rizarry MC, McNamara M, Fedorchak K, Hsiao K, Hyman BT (1997). APPSw transgenic mice develop age-related A beta deposits and neuropil abnormalities, but no neuronal loss in CA1. J Neuropathol Exp Neurol. 56(9):965-973.
- Roberson ED, Scearce-Levie K, Palop JJ, Yan F, Cheng IH, Wu T, Gerstein H, Yu GQ, Mucke L (2007). Reducing endogenous tau ameliorates amyloid beta-induced deficits in an Alzheimer's disease mouse model. Science. 316(5825):750-754.
- Rockenstein E, Mante M, Alford M, Adame A, Crews L, Hashimoto M, Esposito L, Mucke L, Masliah E (2005). High beta-secretase activity elicits neurodegeneration in transgenic mice despite reductions in amyloid-beta levels: implications for the treatment of Alzheimer disease. J Biol Chem. 280(38):32957-32967.
- Rosenbaum G, Cohen BD, Luby ED, Gottlieb JS, Yelen D (1959). Comparison of Sernyl with other drugs: simulation of schizophrenic performance with Sernyl, LSD-25, and amobarbital (Amytal). I. Attention, motor function and proprioception. Arch Gen Psychiatry. 1:651-656.
- Samuel W, Galasko D, Masliah E, Hansen LA (1996). Neocortical Lewy body counts correlate with dementia in the Lewy body variant of Alzheimer's disease. J Neuropathol Exp Neurol 55: 44–52.

- Saura CA, Choi SY, Beglopoulos V, Malkani S, Zhang D, Shankaranarayana Rao BS, Chattarji S, Kelleher RJ 3rd, Kandel ER, Duff K, Kirkwood A, Shen J (2004). Loss of presenilin function causes impairments of memory and synaptic plasticity followed by age-dependent neurodegeneration. Neuron. 42(1):23-36.
- Scheff SW, Price DA (1998). Synaptic density in the inner molecula layer of the hippocampal dentate gyrus in Alzheimer disease. J Neuropathol Exp Neurol 57:1146-1153.
- Schmahmann J.D, Sherman J.C (1998). The cerebellar cognitive affective syndrome. Brain J. Neurol. 121:561–579.
- Schmahmann JD (2004). Disorders of the cerebellum: ataxia, dysmetria of thought, and the cerebellar cognitive affective syndrome. J Neuropsychiatry Clin Neurosci. 16(3):367-378.
- Selkoe DJ (1997). Alzheimer's disease: genotypes, phenotypes, and treatments. Science 275(5300):630-631.
- Selkoe DJ (2001). Alzheimer's disease: genes, proteins, and therapy. Physiol Rev. 81(2):741-766.
- Selkoe DJ (2008). Biochemistry and molecular biology of amyloid beta-protein and the mechanism of Alzheimer's disease. Handb Clin Neurol. 89:245-260.
- Selkoe DJ (2013). The therapeutics of Alzheimer's disease: where we stand and where we are heading. Ann Neurol. 74(3):328-336.
- Sengupta A, Kabat J, Novak M, Wu Q, Grundke-Iqbal I, Iqbal K (1998). Phosphorylation of tau at both Thr 231 and Ser 262 is required for maximal inhibition of its binding to microtubules. Arch Biochem Biophys. 357(2): 299-309.
- Setou M, Nakagawa T, Seog DH, Hirokawa N (2000). Kinesin superfamily motor protein KIF17 and mLin-10 in NMDA receptor-containing vesicle transport. Science. 288(5472):1796-1802.
- Shen J, Kelleher RJ 3rd (2007). The presenilin hypothesis of Alzheimer's disease: evidence for a loss-of-function pathogenic mechanism. Proc Natl Acad Sci U S A. 104(2):403-409.
- Sheng M, Cummings J, Roldan LA, Yan YN, Yan LY (1994). Changing subunit composition of heteromeric NMDA receptors during development of rat cortex. Nature. 368:144-147.
- Shohami E, Biegon A (2014). Novel approach to the role of NMDA receptors in traumatic brain injury CNS. Neurol Disord Drug Targets.13(4):567-573.
- Silva, AJ (2003). Molecular and cellular cognitive studies of the role of synaptic plasticity in memory. J. Neurobiol., 54 (1), 224-237.
- Siman R, Salidas S (2004). Gamma-secretase subunit composition and distribution in the presenilin wild-type and mutant mouse brain. Neuroscience. 129(3):615-628.
- Singh TJ, Haque N, Grundke-Iqbal I, Iqbal K (1995). Rapid Alzheimer-like phosphorylation of tau by the synergistic actions of non-proline-dependent protein kinases and GSK-3. FEBS Lett. 358(3):267-272.
- Singh-Bains MK, Linke V, Austria MDR, Tan AYS, Scotter EL, Mehrabi NF, Faull RLM, Dragunow M (2019). Altered microglia and neurovasculature in the Alzheimer's disease cerebellum. Neurobiol Dis. 132:104589.

- Smith MA, Richey Harris PL, Sayre LM, Beckman JS, Perry G (1997). Widespread peroxynitrite-mediated damage in Alzheimer's disease. J. Neurosci. 17(8):2653–2657.
- Snyder EM, Nong Y, Almeida CG, Paul S, Moran T, Choi EY, Nairn AC, Salter MW, Lombroso PJ, Gouras GK, Greengard P (2005). Regulation of NMDA receptor trafficking by amyloid-beta. Nat. Neurosci. 8 (8), 1051-1058.
- Stella F, Cerasti E, Si B, Jezek K, Treves A (2012). Self-organization of multiple spatial and context memories in the hippocampus. Neurosci Biobehav Rev. 36(7):1609-1625.
- Stokin GB, Goldstein LS (2006). Axonal transport and Alzheimer's disease. Annu Rev Biochem. 75:607-627.
- Stokin GB, Lillo C, Falzone TL, Brusch RG, Rockenstein E, Mount SL, Raman R, Davies P, Masliah E, Williams DS, Goldstein LS (2005). Axonopathy and transport deficits early in the pathogenesis of Alzheimer's disease. Science. 307(5713):1282-1288.
- Sugarman MA, Alosco ML, Tripodis Y, Steinberg EG, Stern RA (2018). Neuropsychiatric symptoms and the diagnostic stability of mild cognitive impairment. J Alzheimers Dis 62(4): 1841–1855.
- Sun L, Zhou R, Yang G, Shi Y (2017). Analysis of 138 pathogenic mutations in presenilin-1 on the in vitro production of Aβ42 and Aβ40 peptides by γ-secretase. Proc Natl Acad Sci U S A. 24;114(4):E476-E485.
- Taffe MA, Weed MR, Gutierrez T, Davis SA, Gold LH (2002). Differential muscarinic and NMDA contributions to visuo-spatial paired-associate learning in rhesus monkeys. Psychopharmacology (Berl). 160(3):253-262.
- Tang YP, Shimizu E, Dube GR, Rampon C, Kerchner GA, Zhuo M, Liu G, Tsien JZ (1999). Genetic enhancement of learning and memory in mice. Nature 401 (6748): 63-69.
- Terwel D, Muyllaert D, Dewachter I, Borghgraef P, Croes S, Devijver H, Van Leuven F (2008). Amyloid activates GSK-3beta to aggravate neuronal tauopathy in bigenic mice. The American journal of pathology. 172(3): 786-798.
- Toyoda H, Li XY, Wu LJ, Zhao MG, Descalzi G, Chen T, Koga K, Zhuo M (2011). Interplay of amygdala and cingulate plasticity in emotional fear. Neural Plast. 2011:813749.
- van de Mortel LA, Thomas RM, van Wingen GA (2021); Alzheimer’s Disease Neuroimaging Initiative. Grey Matter Loss at Different Stages of Cognitive Decline: A Role for the Thalamus in Developing Alzheimer's Disease. J Alzheimers Dis. 83(2):705-720.
- van der Kant R, Goldstein LSB, Ossenkoppele R (2020). Amyloid-β-independent regulators of tau pathology in Alzheimer disease. Nat Rev Neurosci. 21(1):21-35.
- Velazquez R, Ferreira E, Tran A, Turner EC, Belfiore R, Branca C, Oddo S (2018). Acute tau knockdown in the hippocampus of adult mice causes learning and memory deficits. Aging Cell. 17(4):e12775.
- Vertes RP, Linley SB, Hoover WB (2015). Limbic circuitry of the midline thalamus. Neurosci Biobehav Rev. 54:89-107.

- Vezzani A, Serafini R, Stasi MA, Caccia S, Conti I, Tridico RV, Samanin R (1989). Kinetics of MK-801 and its effect on quinolinic acid-induced seizures and neurotoxicity in rats. J Pharmacol Exp Ther. 249(1):278-283.
- Wines-Samuelson M, Schulte EC, Smith MJ, Aoki C, Liu X, Kelleher RJ 3rd, Shen J (2010). Characterization of age-dependent and progressive cortical neuronal degeneration in presenilin conditional mutant mice. PLoS One. 5(4):e10195.
- Wiseman FK, Al-Janabi T, Hardy J, Karmiloff-Smith A, Nizetic D, Tybulewicz VL, Fisher EM, Strydom A (2015). A genetic cause of Alzheimer disease: mechanistic insights from Down syndrome. Nat Rev Neurosci. 16(9):564-574.
- Wong EH, Kemp JA, Priestley T, Knight AR, Woodruff GN and Iversen LL (1986). The anticonvulsant MK-801 is a potent N-methyl-o-aspartate antagonist. Proc Natl Acad Sci U S A. 83(18): 7104-7108.
- Woodruff GN, Foster AC, Gill R, Kemp JA, Wong EH, Iversen LL (1987). The interaction between MK-801 and receptors for N-methyl-D-aspartate: functional consequences. Neuropharmacology. 26(7B):903-909.
- Wozniak DF, Dikranian K, Ishimaru MJ, Nardi A, Corso TD, Tenkova T, Olney JW, Fix AS (1998). Disseminated corticolimbic neuronal degeneration induced in rat brain by MK-801: potential relevance to Alzheimer's disease. Neurobiol Dis. 5(5):305-322.
- Xia D, Watanabe H, Wu B, Lee SH, Li Y, Tsvetkov E, Bolshakov VY, Shen J, Kelleher RJ 3rd (2015). Presenilin-1 knockin mice reveal loss-of-function mechanism for familial Alzheimer's disease. Neuron. 85(5):967-981.
- Xia Y, Prokop S, Gorion KM, Kim JD, Sorrentino ZA, Bell BM, Manaois AN, Chakrabarty P, Davies P, Giasson BI (2020). Tau Ser208 phosphorylation promotes aggregation and reveals neuropathologic diversity in Alzheimer's disease and other tauopathies. Acta Neuropathol Commun. 8(1):88.
- Zanier ER, Bertani I, Sammali E, Pischiutta F, Chiaravalloti MA, Vegliante G, Masone A, Corbelli A, Smith DH, Menon DK, Stocchetti N, Fiordaliso F, De Simoni MG, Stewart W, Chiesa R (2018). Induction of a transmissible tau pathology by traumatic brain injury. Brain. 141(9):2685-2699.
- Zhang H, Wei W, Zhao M, Ma L, Jiang X, Pei H, Cao Y, Li H (2021). Interaction between Aβ and Tau in the Pathogenesis of Alzheimer's Disease. Int J Biol Sci. 17(9):2181-2192.
- Zheng WH, Bastianetto S, Mennicken F, Ma W, Kar S (2002). Amyloid beta peptide induces tau phosphorylation and loss of cholinergic neurons in rat primary septal cultures. Neuroscience. 115(1):201-211.

7. Supplements

7.1 Statistical evaluation:

All evaluations in this study were done by one-way ANOVA. To increase the statistical validity in cases of non-normality of unequal variance, all analyses were also performed as non-parametric ANOVA on Ranks. The results of both tests are provided in the following.

Statistical details Figure 3

(3b)

One-way ANOVA:

PHF1: F = 8.774, d.f. = 4, p < 0.001, n = 5.

ANOVA on Ranks:

PHF1: H = 20.153, d.f. = 4, p < 0.001, n = 5.

Statistical details Figure 4

(4b)

One-way ANOVA:

CP13: F = 5.351, d.f. = 4, p = 0.004, n = 5.

ANOVA on Ranks:

CP13: H = 8.913, d.f. = 4, p = 0.063, n = 5.

Statistical details Figure 5

(5b)

One-way ANOVA:

Tau-1: F = 4.000, d.f. = 4, p = 0.015, n = 5.

ANOVA ON RANKS:

Tau-1: H = 10.782, d.f. = 4, p = 0.029, n = 5.

Statistical details Figure 6

(6a)

One-way ANOVA:

PHF1: F = 6.923, d.f. = 4, p = 0.001, n = 5.

ANOVA on Ranks:

PHF1: H = 20.485, d.f. = 4, p < 0.001, n = 5.

(6b)

One-way ANOVA:

CP13: F = 3.740, d.f. = 4, p = 0.020, n =5.

ANOVA on Ranks:

CP13: H = 9.327, d.f. = 4, p = 0.053, n = 5.

Statistical details Figure 8

(8b)

One-way ANOVA:

PHF1: F = 5.009, d.f. = 4, p = 0.006, n = 5.

ANOVA on Ranks:

PHF1: H = 14.341, d.f. = 4, p = 0.006, n = 5.

Statistical details Figure 9

(9b)

One-way ANOVA:

CP13: F = 62.030, d.f. = 3-4, p < 0.001, n = 4-5.

ANOVA on Ranks:

PHF1: H = 14.949, d.f. = 3-4, p = 0.002, n = 4-5.

Statistical details Figure 10

(10b)

One-way ANOVA:

Tau-1: F = 13.101, d.f. = 3-4, p < 0.001, n = 4-5.

ANOVA on Ranks:

Tau-1: H = 17.961, d.f. = 3-4, p = 0.001, n = 4-5.

Statistical details Figure 11

(11a)

One-way ANOVA:

PHF1: F = 9.061, d.f. = 4, p < 0.001, n = 5.

ANOVA on Ranks:

PHF1: H = 16.763, d.f. = 4, p = 0.002, n = 5.

(11b)

One-way ANOVA:

CP13: F = 36.067, d.f. = 4, p < 0.001, n = 4.

ANOVA on Ranks:

CP13: H = 15.303, d.f. = 3, p = 0.002, n = 4.

Statistical details Figure 12

(12b)

One-way ANOVA:

PHF1: F = 8.092, d.f. = 4, p < 0.001, n = 5.

ANOVA on Ranks:

PHF1: H = 17.908, d.f. = 4, p = 0.001, n = 5.

Statistical details Figure 13

(13b)

One-way ANOVA:

CP13: F = 1.325, d.f. = 4, p = 0.295, n = 5.

ANOVA on Ranks:

CP13: H = 9.046, d.f. = 4, p = 0.060, n = 5.

Statistical details Figure 14

(14b)

One-way ANOVA:

Tau-1: F = 6.930, d.f. = 4, p = 0.001, n = 5.

ANOVA on Ranks:

Tau-1: H = 14.385, d.f. = 4, p = 0.006, n = 5.

Statistical details Figure 15

(15a)

One-way ANOVA:

PHF1: F = 6.685, d.f. = 4, p = 0.001, n = 5.

ANOVA on Ranks:

PHF1: H = 16.844, d.f. = 4, p = 0.002, n = 5.

(15b)

One-way ANOVA:

CP13: F = 1.501, d.f. = 4, p = 0.240, n = 5.

ANOVA on Ranks:

CP13: H = 9.135, d.f. = 4, p = 0.058, n = 5.

Statistical details figure 16

(16b)

One-way ANOVA:

PHF1: F = 6.548, d.f. = 3, p = 0.004, n = 4.

ANOVA on Ranks:

PHF1: H = 11.411, d.f. = 3, p = 0.010, n = 4.

Statistical details figure 17

(17b)

One-way ANOVA:

CP13: F = 0.593, d.f. = 3, p = 0.629, n = 4.

ANOVA on Ranks:

CP13: H = 1.900, d.f. = 3, p = 0.593, n = 4.

8. Note of thanks

I would like to take this opportunity to express my gratitude to my supervisor, Prof. Dr. Moosmann, for his encouragement and guidance throughout every step of this study. Without your support, it would not have been possible to complete this dissertation.

I would also like to thank the entire working group of Prof. Dr. Moosmann for their assistance and support during my work in the laboratory.

Finally, I extend my heartfelt appreciation to Prof. Dr. Kristina Endres reviewing my dissertation and for her valuable feedback and insights.

Thank you all for your support and encouragement.

Sincerely,

Alan Souid

9. Curriculum Vitae

ALAN SOUID

AUSBILDUNG

2018 – 2024	Studium der Humanmedizin an der Johannes-Gutenberg-Universität Mainz
2017 – 2018	Deutschkurs in der Sprachakademie „Perfekt Deutsch“ in Dortmund
2015 – 2017	Studium der Humanmedizin an der Albaath Universität in Homs, Syrien
2012 – 2015	Allgemeine Hochschulreife, Almozeina-Gymnasium in Homs, Syrien, Abitur: 1,1

AUSZEICHNUNGEN

2020 – 2024	Stipendiat der Friedrich-Ebert-Stiftung

BERUFSERFERFAHRUNG

2025 – Aktuell	Assistenzarzt in der HNO-Klinik, GPR - Rüsselsheim
2021 – 2025	Medizinischer Doktorand am Institut für Pathobiochemie der Universitätsmedizin Mainz
2021 – 2023	Studentische Hilfe in der Abteilung Orthopädie und Unfallchirurgie, MKM Mainz
2020 – 2021	Wissenschaftliche Hilfskraft im Studienzentrum der Angiologie, Universitätsmedizin Mainz
2019 – 2020	Studentische Aushilfe im Schlaflabor, DRK-Krankenhaus Alzey

EHRENAMTLICHES ENGAGEMENT

2021 – heute	Bildungsnetzwerk (BINE) Mainz
2019 – heute	Landesverband der syrischen Akademiker in Rheinland-Pfalz

SPRACHEN

Deutsch (Experten-Kenntnisse / C1-C2)

Englisch (sehr gute Kenntnisse / B2-C1)

Arabisch (Muttersprache)